MULTIVATOR DESIGN STUDIES

September 1965

Prepared for
The National Aeronautics and Space Administration
Grant NsG 81–60

Design Division
Department of
Mechanical Engineering
Stanford University
Stanford, California

INTRODUCTION

The following reports were prepared under NASA Grant 81-60, Cytochemical Studies of Planetary Micro-Organisms, by graduate students in the Design Division of the Department of Mechanical Engineering. The reports represent concentrated studies of specific problems encountered during the design of Multivator, an instrument for the detection of extra-terrestial life. In addition to expanding the store of technology regarding automated biological instrumentation, the topics covered have provided an educational experience for the students involved.

The first report, Soil Sampling on Mars for Life Detection, deals with the problems of sample collection and includes a discussion of laboratory techniques which would be useful in the development of a sampling device. The second report, A Pneumatic Soil Sample Collector, describes a sample collector which would be useful primarily for Earth-based testing of life detection instruments requiring the input sample in the form of an aerosol. The collector design has sufficient merit to be considered as a possibility for localized sampling of the Martian terrain.

The third report, Delivering and Metering Minute Quantities of a Liquid, was prepared when it was realized that small volumes of reagents on the order of microliters or less could be involved in the processes of an automated wet chemistry laboratory.

The fourth and fifth reports, Miniature D.C. Solenoids, and Evaluation of the Hercules BA 31 K7 Motor, were part of an investigation into the types of mechanical actuators suitable for use in an application placing a premium on low weight and high energy density.

The sixth report, Feasibility of a Spur Gear Train for Operating a Rotary Valve, was a study of the problems encountered in driving a high-friction, sliding disc valve of the type used in gas chromatography or in controlling complex, multi-path flows as encountered in automated wet chemistry systems.

The seventh report, Analysis of a Multivator Module, was an investigation into the dynamic characteristics of a pneumatically-actuated version of the Multivator in order to determine the effects of pressure levels and geometry on its performance. The information acquired will support the development of similar devices where optimization could result in lower energy requirements and increased reliability.

SOIL SAMPLING ON MARS
FOR LIFE DETECTION

Prepared by W. F. Lapson
Research Associate

May 31, 1965

Prepared Under

National Aeronautics and Space Administration
Grant NSG-8160

Design Division
Department of Mechanical Engineering
Stanford University
Stanford, California

I. Introduction

A soil sample is the primary input to most of the life detection instruments proposed to date since it is believed that if life exists on Mars, the most common and easily acquired organisms will be soil-dwelling microbes.

In general, the design of a Martian soil sampler is dictated by the quantity of sample required and the terrain from which the sample is taken. Some life-detection tests, such as those based on enzyme activity or bacteria growth require only a few milligrams of sample. Other experiments may require several grams of sample, particularly when sample enrichment techniques are to be used to increase sensitivity. Samples may be taken from terrain ranging from sandy stretches, pebble-strewn desert pavements, to rocky mountain slopes.

Since microbes are small and have lower density than most rock, it is likely that a sample collection system will be required to assort particles according to size and density in order to reduce the amount of inert material in the sample.

The preceding discussion identifies the reason for soil sampling and some of the associated problem areas. What follows is an elaboration on the nature of the sampling problem and some possible solutions.

II. The Martian Environment and Possible Life Forms

The design of a sample collecting system for a Martian life detection instrument must take into account such factors as climate, terrain, probable life forms and their distribution.

The temperatures on Mars range from -75°C at night to 22°C at noon. The atmosphere is quite rarified with a pressure at the surface somewhere in the range of 10 to 100 millibars. The predominant constituent of the atmosphere is nitrogen, about 94%, with $O_2<0.1\%$, and $H_2O<0.1\%$. Due to the low atmosphere pressure, water usually exists either as ice or vapor, although at 10 mb pressure and 8°C water can exist as a liquid.

Most of the planet's surface appears to be covered with bright reddish or orange areas usually referred to as deserts or continents. These areas are probably covered with dust deposits formed from rock resembling the Earth minerals, limonite and felsite. Dark areas are seen as a pattern of maria, canals, and oases. There are changes in the outline and intensity of the dark regions randomly and seasonally which may be caused by the presence of living organisms. However, the dark areas may also be the result of winds stripping away dust deposits and revealing dark rock surfaces.

The dominant erosive agent is probably wind action although ice wedging in the polar regions and fatigue due to the extreme daily temperature variations may be of some account. Wind velocities are estimated to range from 5 to 35 mph as based on observations of yellow dust cloud movements.

The desert areas might consist of flat plains covered with a mosaic of pebbles and large rocks with fine particles either swept away by the wind or lying beneath a surface of larger rock particles.

Biologists presently believe that if life exists on Mars it will most likely be uni-cellular in its more common forms. Organisms will probably exist near the surface where there is an opportunity to capture water when it is deposited as frost or condensation. Life forms will have to be rugged to withstand wind abrasion, ultra-violet radiation, dune burial, and great temperature extremes. The organisms will probably be found adhering to rock particles. If Mars and Earth organisms are analogous, the Martian organisms will probably have specific densities of 1.2 as compared to 1.4 for rock and will range in size from 1 to 20 microns in diameter.[2] Bacteria counts of Earthly soil samples indicate that the number of bacteria in a sample are directly proportional to the total particle surface area per gram; consequently, samples containing small particle sizes (e.g.<100 microns diameter) will probably yield the most organisms for analysis.

Due to the scarcity of water in liquid form, muddy samples are not expected. However, the soil may be compacted and frozen into a solid due to the presence of moisture.

The low environmental temperature and pressure imply that special precautions will have to be taken to prevent freezing or evaporation of any liquids used in the sampling device. The same considerations can also be used to advantage if necessary. For example, particle fractionation can be accomplished in a water suspension with subsequent removal of the water by evaporation.

III. Particle Collection, Transport, and Fractionation

A. Particle collectors can operate on the basis of adhesion, air movement, or mechanical motion. For example, adhesive surfaces produced by sticky coatings or electrostatic charges have been developed. Vacuum cleaners, and rotating brushes that sweep the particles into a scoop are other possible means for collecting particles.[15]

A miniature vacuum cleaner, devised at the General Mills Corporation, is intended to be carried over the Martian surface on inflated balloon tires at distances up to 10 feet from the main instrument package.[12] Dust particles picked up at the intake are pneumatically propelled through a hose into the main instrument package where they are collected. A motor-driven blower provides the required vacuum. The device can pick up 0.2 grams per minute of particles ranging in size up to 100 microns in diameter with a power consumption of 5 watts. The wheels and connecting hose are collapsible in order to minimize the storage volume.

The Gulliver life detection instrument makes use of chenille strings, or grease coated strings, which pick up particles as the strings are dragged over the ground.[16] In operation, a projectile containing a spool of string is fired away from the instrument while one end of the string remains fastened to a motor-driven drum in the instrument. After the projectile lands, the strings are reeled in. The string collector works well since it does not have to be oriented in any particular position on the surface in order to operate properly, and, being light weight, it moves easily over obstructions.

A particle collection system designed at JPL consists of an electrostatically charged plastic strip which attracts particles as it is dragged over the surface.[15] The plastic strip is actually a flattened tube which is initially wrapped on a drum. The tube is inflated, causing it to shoot across the ground in the manner of a party favor. As the charged strip is reeled in by means of a motor, the particles are scraped into a trough.

A dust collector used with the field-test version of the Multivator, consists of an inverted funnel with air jets at the base and a pneumatic aspirator at the top.* In operation, the air jets create an aerosol which causes large particles to swirl around the base continuously while finer particles rise to the top where the aspirator propels them pneumatically into the instrument proper.

An experimental dust collector designed at Litton Industries is simply a shallow open box with a brush on one edge, air jets inside the box, and a tube connecting the collecting head to the instrument proper.[13] In operation, the open side of the box is placed on the ground and dragged over the surface. The brush scours particles from the surface while the air jets cause the particles to form a cloud which is then picked up by a pneumatic aspirator.

A simple means for collecting particles might consist of a mat laid on the ground and periodically rolled in to collect wind-borne particles which may have settled on it. A funnel mounted on a weather-vane might also be used to capture wind-borne particles.

B. Particle Transport

Once the particles have been collected, they can be transported to the processing centers by direct mechanical motion, e.g., a conveyor belt, or in the form of an aerosol. The transport of particles in the form of an aerosol requires velocities high enough to prevent particles from settling out in the transporting tube. Since air flow is directly related to electrical power consumption when a blower is used, or to the size of a compressed air storage vessel, it is worthwhile optimizing the air flow required for transporting particles in a given size range.

Theoretically, the critical velocity for conveying a particle upwards in air is slightly greater than its terminal velocity while falling in air. Consequently, if the terminal velocity of the largest particle to be transported is calculated, this will form a basis for estimating air flow requirements. The terminal velocity of a falling spherical particle in the Martian atmosphere can be calculated using Stoke's equation:

*See Figure 1.

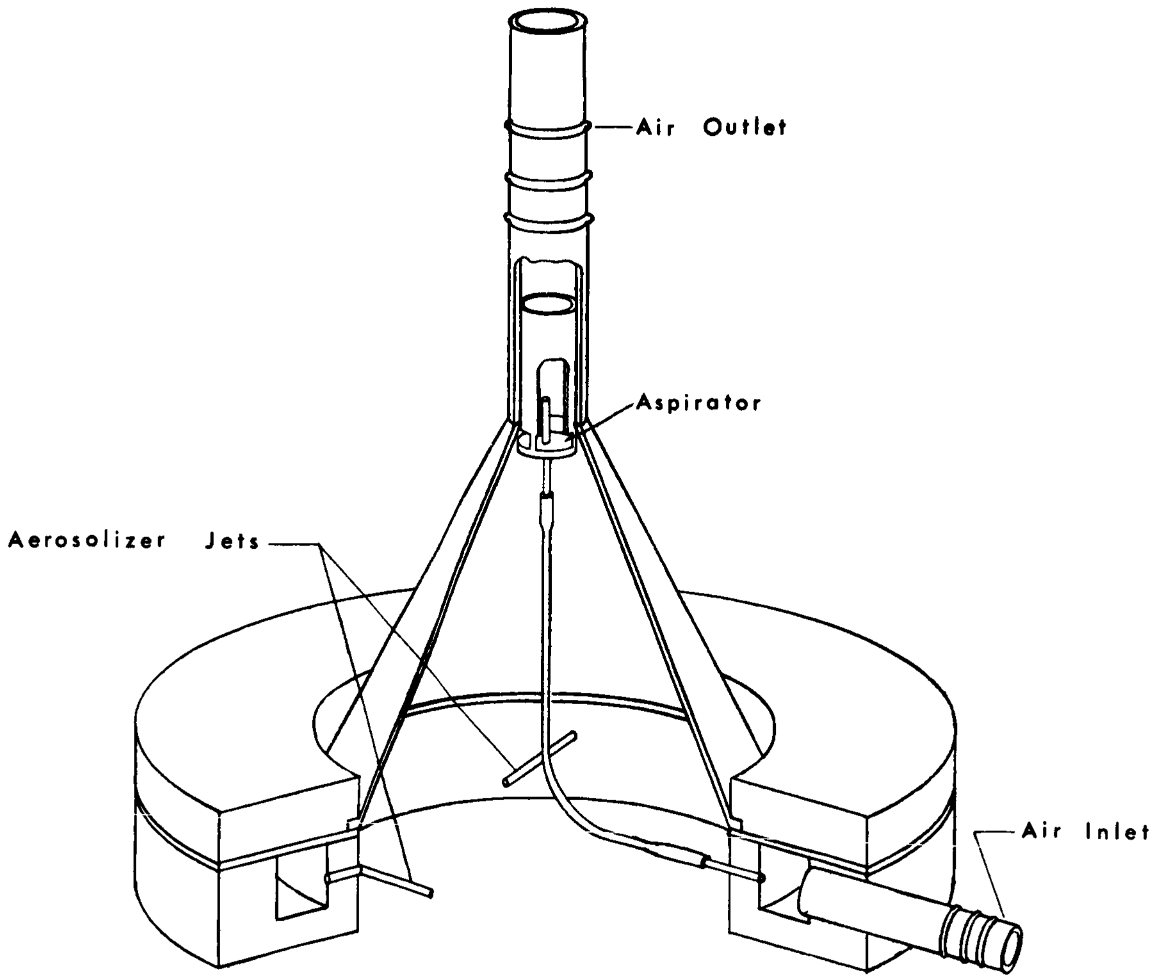

Figure 1: Soil Sample Collector

(1)

$$v = \frac{2\ gr^2(\rho-\rho')}{9\eta}$$

g = acceleration of gravity

ρ = density of particle

ρ' = density of air

η = viscosity of fluid

r = radius of particle

v = terminal velocity

If $\rho' \ll \rho$, then equation (1) reduces to

(2)

$$v = \frac{2gr^2\rho}{9\eta}$$

A sample calculation will indicate the velocity required to transport 100 micron diameter particles on Mars.

$g = 370\ \text{cm/sec}^2$

$\rho = 1.5\ \text{gm/cm}^3$

ρ' = negligible

$\eta = 1.4 \times 10^{-4}\ \frac{\text{gm}}{\text{cm.sec}}$ (88.5 mb, -75°C)

$r = 50 \times 10^{-4}\ \text{cm}$

$$v = \frac{(2)(370)(50\text{x}10^{-4})^2(1.5)}{9\text{x}1.4\text{x}10^{-4}} = 22\ \frac{\text{cm}}{\text{sec.}}$$

$$v = 43.4\ \frac{\text{ft}}{\text{min.}}$$

Consideration of Stoke's equation shows that the transported particle diameter is proportional to $\sqrt{v}$, and therefore not a sensitive function of the air velocity. Consequently, to assure maximum particle transport, the velocity should be markedly increased over the minimum required. Pneumatic particle conveying systems in industrial applications typically use velocities several times the terminal velocity of the largest particle.

A second consideration for the required air velocity is based on the boundary layer thickness in horizontal conveying tubes. A problem with horizontal tubes is that particles can settle out of the air stream into the stagnant boundary layer. High Reynolds Numbers corresponding to high flow velocity would probably minimize the problem of settling during transport.

C. Separation of Particles from the Air Stream

Assuming that the dust particles are pneumatically conveyed from the collection head to the instrument proper, it is necessary to separate the particles from the air stream. Separation can be achieved by several means listed as follows:

1. Filtration
2. Cyclone separation
3. Settling
4. Electrostatic precipitation
5. Thermal precipitation
6. Impingement
7. Centrifugal separation

1. Filtration

In using filtration, sufficient filter area must be used to assure low flow resistance as the particles accumulate on the filter surface. The following calculation will give an indication of the area required to maintain low flow resistance, and, consequently, pumping power.

The pumping power is given by the following equation:

(2)

$$P = Q\Delta p$$

Q = volumetric flow rate

Δp = pressure drop across filter

The pressure drop is a function of the filter flow resistance, flow rate, and filter area,

(3)

$$\Delta p = \frac{QR}{A}$$

The pumping power is found by combining equation (2) and (3),

(4)
$$P = (Q)\left(\frac{QR}{A}\right)$$
$$P = \frac{Q^2R}{A}$$

We shall assume that Millipore filter paper is used with an 8 micron pore size.[17] This type of filter paper has unusually low flow resistance for retaining particles of a given size. According to the calculations in the preceding section on particle transport, a flow velocity of 80 ft/sec in a tube 3/16 diameter should transport particles below 100 microns. This corresponds to a flow rate of 0.015 ft^3/sec. The flow resistance of Millipore filter paper is 64.6 lb sec/ft^3 at 88 millibars pressure. Assuming that the pumping power shall be limited to one watt initially, the filter area required is,

$$A = \frac{Q^2R}{P}$$
$$Q = 0.015 \ ft^3/sec$$
$$R = 64.6 \ lb.sec/ft^3$$
$$P = 1 \ watt = 0.738 \ ft.lb/sec$$
$$A = \frac{(0.015)^2(64.6)}{(0.738)}$$
$A = 1.97 \times 10^{-2} ft^2$ (roughly equivalent to a 1 inch diameter disc)

2. Cyclone Separation

Cyclone separators of the type shown in Figure 2 utilize centrifugal force to separate particles from the air stream. In operation, dust-laden air enters the cylindrical section of the separator tangentially and at high velocity. A vortex is formed in which particles are propelled against the walls and fall to the lower end of the cone while clean air travels up and out the top.

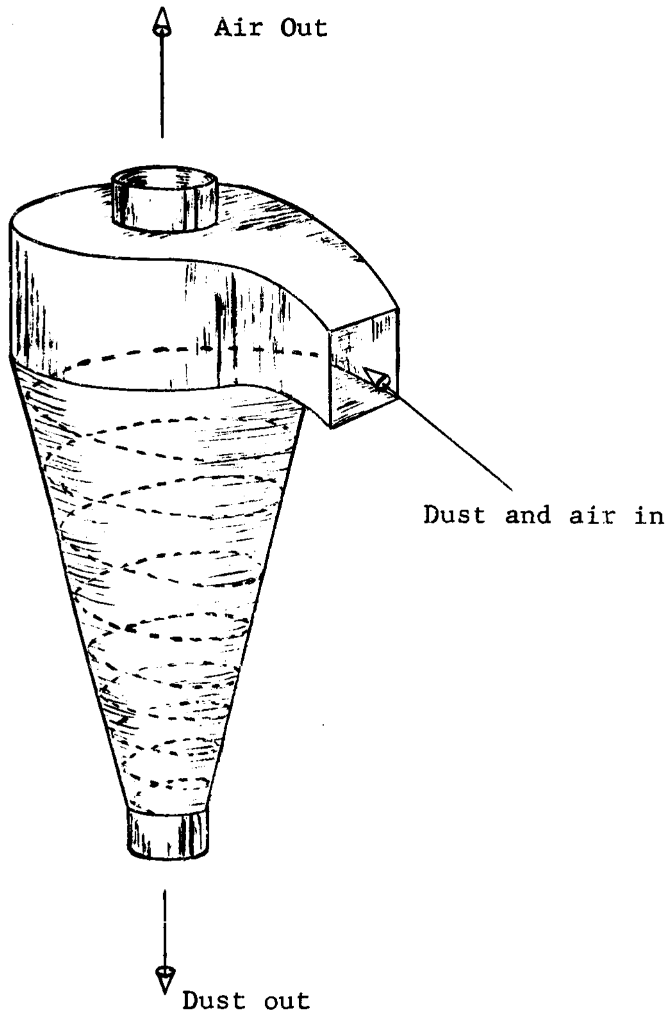

Figure 2: Cyclone Separator

The centrifugal settling velocity, which is the radial velocity of a dust particle, is expressed by the following equation:

$$v_c = \frac{\alpha_v d^2 g}{K} \frac{(\rho - \rho_o)}{\mu} \frac{v_t^2}{R} \qquad (5)$$

This equation is a modification of Stoke's equation given in the same reference[11] as,

$$v = \frac{\alpha_v d^2 g}{K} \frac{(\rho - \rho_o)}{\mu} \qquad (6)$$

v_t = tangential velocity of inlet air
v = terminal velocity of particle
v_c = centrifugal settling velocity
d = particle diameter
g = acceleration due to gravity
K = 3Π for spheres
ρ = density of particle
ρ_o = density of fluid
α_v = constant where $\alpha_v d^3$ = volume of particle
μ = viscosity of fluid
R = radius of circular path of particle

A comparison of equations (5) and (6) shows that

$$v_c = v \times \frac{v_t^2}{Rg} \qquad (7)$$

The factor $\frac{v_t^2}{Rg}$ is called the separation factor, and is a measure of the increase in separation resulting from using centrifugal action to augment gravitational action.

A sample calculation will illustrate the utility of the cyclone separator. Assume that the tangential inlet velocity is 30 ft/sec. and the radius of the separator is 2 inches.

The value of g on Mars is about 12 ft/sec^2.

$$\frac{v_t^2}{Rg} = \frac{(30)^2}{(1/6)(12)} = 450$$

The cyclone separator could thus cause particles to settle out of the air in 1/450th of the time it would take for them to settle out of still air.

3. Settling Chamber

Settling chambers depend entirely on gravitational forces for their operation and consequently are not efficient for separating small particles which settle very slowly. The settling chamber must be large enough so that the inlet air velocity is quickly dissipated to a negligibly low value.

4. Electrostatic Precipitation

Electrostatic precipitation is known to be particularly effective in collecting fine dust particles down to sub-micron size.[6,11] Collectors of this type make use of a corona discharge to induce a charge on the particles to be collected. The charged particles are then attracted to a surface with an opposing charge. A practical electrode configuration consists of a cylinder, the anode, with a concentric wire cathode. The dust is blown through the tube and impinges on a charged metal plate where the particles adhere. Potentials used in electrostatic collectors may range from 5 to 100 KV. The collection efficiency when working with dry, non-conductive dusts can be improved by moistening the particles with water vapor.

5. Thermal Precipitation

Thermal precipitation has been used as a means for collecting dust particles.[6] This technique is based on the fact that the air molecules near a heated surface have a preferred direction of motion away from the surface. Consequently, if air containing dust particles is passed between two surfaces, one heated and the other cool, the air molecules will tend to be repelled from the hot surface toward the cold surface and in so moving will impact the dust particles against the cold surface.

Thermal precipitators are considered to be efficient, particularly for collecting particles in the sub-micron size range. They have the disadvantage of being relatively slow, although thermal precipitators have been made which can handle one liter of air per minute.

An equation has been developed relating the thermal force on a spherical particle reproduced as follows:[6]

$$F_t = -9\pi r \frac{k_a}{2k_a + k_i} \frac{\eta^2 G}{\rho T} \quad (8)$$

F_t = thermally produced force

r = radius of spherical particle, cm.

k_a = thermal conductivity of the gas, cal/cm sec °K

k_i = thermal conductivity of spherical particle, cal/cm sec °K

η = viscosity, poises

ρ = density of air, g/cm^3

T = absolute temperature, °K

G = temperature gradient, °K/cm

6. Impactors and Impingers

The operation of impactors and impingers is based on the fact that if air containing a particle suspension is passed through a nozzle and the resulting jet is directed at a surface, the direction of air flow changes abruptly at the surface. Particles in the air stream, however, continue toward the surface due to their momentum and will cling to the surface if the surface is sticky or wet or as a result of intermolecular forces in the case of very small particles. Separators of this type have characteristically high collection efficiencies, approaching 100% for particles down to 0.6 microns, and collect particles in a sharply defined size range[6]. It is possible to construct an impinger type dust collector with several stages of nozzles in series, each successively smaller in diameter. The result is a collector which separates the incoming dust particles into size fractions.

7. Centrifugal Separation

Centrifugal dust separators resemble impactors in principle. A centrifugal blower augments the velocity of the incoming air stream and propels the air and dust particles in an outward, radial direction toward a collection chamber as shown in Figure 3. The air path curves sharply immediately in front of the collection chamber so that dust particles continue along a radial path into the chamber while the air completes the curve and is exhausted. There is no air flow through the collection chamber. A centrifugal dust collector was successfully used on one version of the Multivator.

In industrial applications the efficiency of this type of collector is sometimes improved by recirculating through the blower some of the air from the dust collection chamber and by adding a water spray to the incoming air so that the dust is handled as a sludge.[11]

D. Particle Fractionation According to Size or Density

Microbes on Earth are typically of a size ranging from 1 to 20 microns in diameter with a specific density of 1.2 as compared to 1.4 for typical rocks.[2] Assuming that Martian bacteria fall in a similar size range and have a characteristic density, then we have a means for differentiating the bacteria from the inert surrounding material.

The separation of inert soil particles from bacteria according to density can be achieved using flotation methods. To illustrate, the sample is placed on the surface of a solution having a density less than that of the inert, rocky material but greater than that of the bacteria. The result is that rock particles will eventually settle

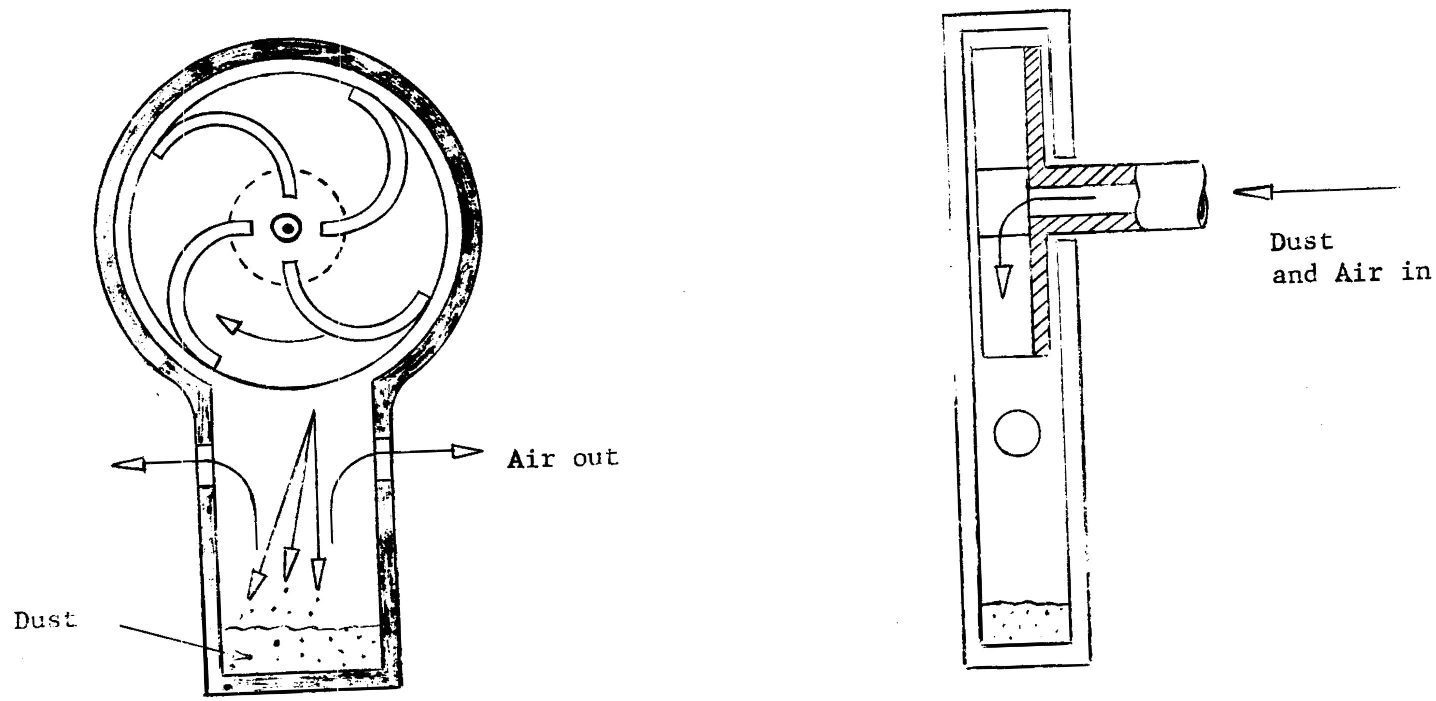

Figure 3: Centrifugal Dust Separator

to the bottom of the solution while the bacteria remain floating on the surface where they can be decanted.

A variation of the flotation technique known as density gradient centrifugation can separate a sample into density fractions. In this method a centrifuge is filled with a solution of varying density where the density is greatest at the outermost radius and decreases toward the center of rotation. A suspension of the soil sample is layered on the surface of the density gradient solution and then centrifuged. After some time, all particles reach an equilibrium position where the particle density is equal to the density of the surrounding fluid.

A disadvantage of flotation techniques is that a large proportion of the bacteria may adhere to the inert particles and would therefore be removed along with these particles. Attempts have been made to remove bacteria from soil particles by sonification and the addition of chemicals or detergents to a suspension which have the effect of releasing the bacteria.

Particle size fractionation can be achieved by several means, the most practical being; sieving, sedimentation, elutriation, and multi-stage impaction. Multi-stage impaction was mentioned in the preceding section describing collecting techniques. The other size fractionating methods will be covered in the next section which describes laboratory measurements of particle size.

IV. Particle Size Determination in the Laboratory

A. Introduction

The development of soil sampling systems for Martian life detection instrumentation requires a good knowledge of the various techniques used in particle size analysis. Some of the more applicable techniques will be described in the following sections, in addition to a discussion of the various criteria used to define particle size.

Particles are usually irregular in shape and rarely spherical, however, certain parameters can be decided upon as a definition of particle size. For example, the diameter of a particle can be defined as the arithmetic mean of the length, breadth, and thickness of the particle. Assuming the particle is resting on a horizontal plane in the position of greatest stability, the breadth is defined as the distance between two parallel lines tangent to the projection of the particle on the plane and placed so that the distance between them is as small as possible. The length is the distance between two parallel lines tangent to the projection and perpendicular to the lines defining breadth. The thickness is defined as the distance between two horizontal planes tangent to the top and bottom surfaces of the particle.[6] Several other definitions of particle diameter are the following:

(1) The diameter of a particle is equal to the diameter of a circle having the same area as the projected area of the particle when the particle is in its most stable position.

(2) Particle diameter can be based on the figure obtained by projecting an image of the particle onto a plane surface. A line drawn between opposite sides of the particle and bisecting the projected area is defined as the particle diameter.

(3) An easy to apply definition of particle diameter when making microscope measurements is that particle diameter is the distance between two tangents to the particle.

(4) Particle diameter is sometimes defined as the diameter of a spherical particle which has the same dynamic characteristics as the irregular particle. The diameter can be calculated by observing the fall of the particles in a fluid and making use of Stoke's Law for spherical particles. Similarly, the diameter of a particle can be based on the results of tests using standardized sieves.

(5) When an accurate description of particle shape is important, a microphotograph is the best solution. Such factors as flakiness, crystallinity, sphericity, and color are easily described by a photograph.

B. Microscopy

An optical microscope is useful for particle size determinations in the range of 0.2 to 100 microns. The lower limit of resolution of a microscope using visible light is 0.2 microns; however, by using ultra-violet light and a fluorescent screen or photographic film to render an image, measurements can be made down to 0.1 microns. An electron microscope is more practical than an ultra-violet microscope when measuring particles 0.2 microns or less in diameter.

Measurements can be made with the microscope by means of an ocular micrometer which is a transparent scale placed in the focal plane of the ocular. The ocular micrometer is calibrated by means of a stage micrometer with linear rulings.

The thickness of a particle can be measured by focusing first on the top and then the bottom of the particle. The thickness of the particle is then determined by the amount of rotation of the fine-focusing knob which must be graduated. Calibration of the fine-focusing knob graduations is accomplished using a fine fiber of known diameter.[7]

An indirect way of measuring particle size is to photograph the particle sample and make measurements on an enlargement. A disadvantage of photomicrography is that the particles may not be in as sharp focus as when direct observations are made as a result of the eye being more accommodating than the camera and also because focus can be adjusted during direct measurements.

Micro-projection apparatus can also be used for measuring particle size and determining size distribution. In this technique, an intense light source is used to project an image of the particles onto a screen.

The selection of a sample prior to determining particle size distribution by microscopy is of critical importance. If the particle size range is very wide, there may be hundreds of small particles for each of the large ones. In this event, the sample should be divided into size classes, each of which is analyzed separately.[6]

A slide can be prepared by first coating it with an invisibly thin layer of vaseline. A tube is vertically positioned over the slide and a pinch of the sample is dropped in the upper end of the tube. The particles will then settle in a uniformly thick layer on the slide.

Particles in a liquid suspension can be conveniently counted and sized by placing the sample in a hemacytometer cell.

C. Sedimentation

The sedimentation velocity of small particles in liquids or gases can be used as a basis for determining the size distribution of particulate material ranging in size from 2 to 50 microns. Sedimentation techniques can also be used to separate the material into size fractions.

Sedimentation tests often start with a uniform suspension of particles in a tall vessel. At successive time intervals, the total amount of material remaining in suspension above a certain level is determined. Alternately, the total amount of material which has settled below a certain level can be determined. The results are plotted as a weight versus time curve. The problem of calculating the size distribution from this curve can be solved as follows,[6]

Let h = the settling distance

W = total fraction sedimented at time t

w = the fraction consisting of particles whose settling times for the distance h are equal to or less than t

t = time at which weight W is determined.

The equation governing the sedimentation process is,

$$(9) \quad W = w + t_w \frac{dw}{dt}$$

The desired quantity, w, can be obtained from the W vs. t curve by a graphical analysis, as shown in Figure 4.

The size of particles having a falling time of a given value can be determined using Stoke's equation. The falling velocity v_w is given by,

$$(10) \quad v_w = \frac{h}{t_w}$$

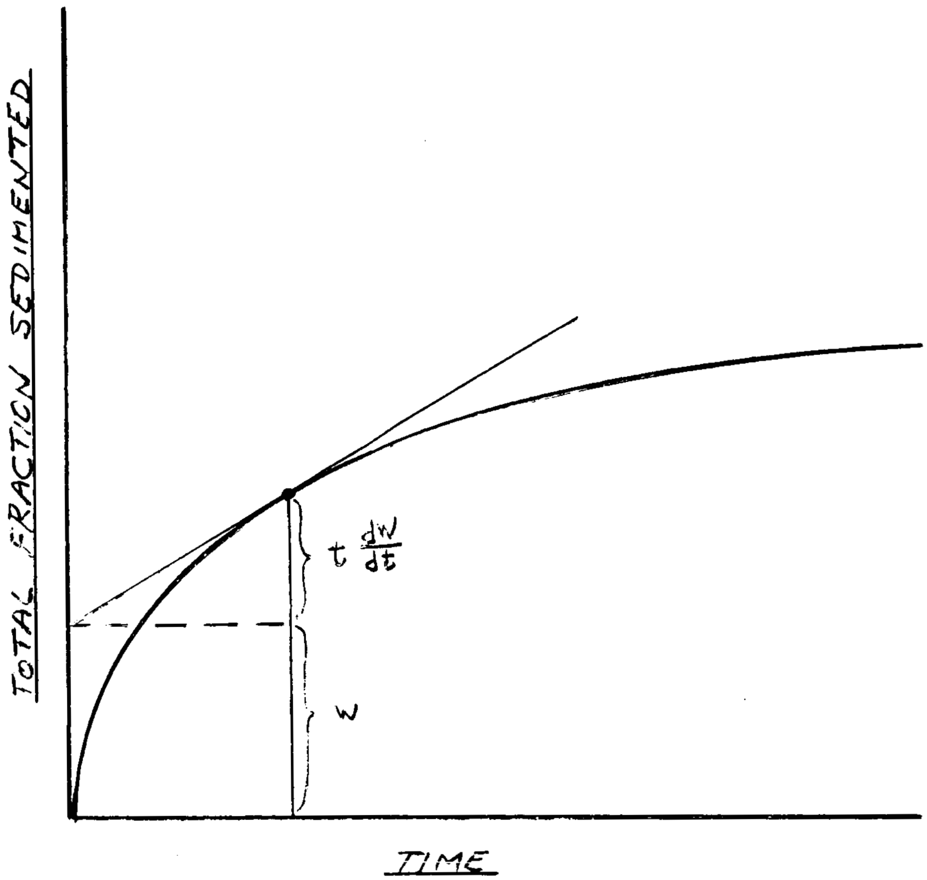

Figure 4: Intercept Method for determining $t\frac{dw}{dt}$ and w.

Equation (10) can be related to Stoke's equation for spherical particles,

$$(1) \quad v_w = \frac{2gr_w^2(\rho - \rho')}{9\eta}$$

(See page for definition of symbols)

The particle radius can be found by equating (1) and (11) and solving for r_w,

$$(11) \quad r_w = \frac{9\eta h}{2g(t_w)(\rho - \rho')}$$

The total weight fraction, W, can be determined by placing a balance pan at the bottom of the column. Single-pan, substitution type balances are well suited for this purpose since the pan oscillates very little during a weight determination, and weight can be determined quickly.

Another technique for determining size fractions involves placing a liquid suspension of dust particles on the surface of a clear liquid column. The concentration of particles at a particular level is then determined at regular time intervals by drawing off a sample with a pipette. The sample is placed in an evaporating dish and the remaining particles are weighed.

An important consideration in conducting sedimentation tests is the choice of fluid. The fluid should be sufficiently viscous so that the Reynold's Number is less than 1, which is a requirement for Stoke's equation to be accurate. For higher Reynold's Numbers, a form of Stoke's equation including the Cunningham slip correction factor must be used. However, the fluid should not be so viscous that the test will be excessively prolonged. Another consideration is that the fluid should not dissolve the particles or chemically react with them. Some commonly used fluids are water, alcohol, mixtures of acetone and vegetable oil, mixtures of glycerol and water, and air. When water is used as the suspending medium, salts or wetting agents may be added to prevent clumping or coagulation of the particles. Some commonly used salts are sodium pyrophosphate, calcium chloride, or potassium citrate used in 0.1 mole concentrations or less. Microscopic examination of a drop of suspension will reveal whether coagulation is occurring.

Particle concentrations of about 1% of the fluid volume are usually used to assure accurate results.

Sedimentation methods depending solely on gravitational forces are limited to determining the size distribution of particles 2 microns or larger in diameter. Sedimentation times for smaller particles may be excessively long or in error due to convective currents and Brownian movement effects. Centrifugation can be used to extend the range of sedimentation tests down to 0.05 microns. A modification of Stoke's equation relates particle diameter to the centrifugation parameters as follows:[6]

$$(12) \quad d = \frac{6}{\omega}\left[\frac{\eta \log_e \frac{S_2}{S_1}}{2(\rho - \rho')t}\right]^{\frac{1}{2}}$$

ω = angular velocity of centrifuge

S_1 = distance from center of rotation to the

S_2 = distance from center of rotation to the bottom of centrifuge tube

η = fluid viscosity

ρ = particle density

ρ' = fluid density

t = time interval of centrifugation

d = particle diameter

For a given set of experimental conditions, equation (12) reduces to

$$d = \frac{\text{constant}}{\sqrt{t}}$$

D. Elutriation

Elutriation methods for size fractionation involve passing a stream of fluid upward through a bed of particles. Depending on the flow velocity, particles of a given size will remain suspended in the stream while larger particles settle and smaller particles follow the flow.

The elutriating fluid can be a liquid or gas. Particles may be removed from the fluid stream by filtration, or if the fluid is a gas, by impaction. If the process is carried out in steps using successively higher fluid velocities, the sample can be divided into fractions according to particle size.

Elutriation is the opposite of sedimentation but is also based on Stoke's equation for falling particles and consequently measures the same characteristics. The fluid velocity for suspending particles of a given size is equal to the terminal velocity for particles of the same size falling in the fluid. This velocity can be calculated using Stoke's equation.

E. Sieving

Sieving methods involve taking the sample and passing it through sieves of various standard meshes. The sample is usually dry and is caused to flow through the sieve by tapping or vibrating the latter. Sieving methods are not ordinarily used for separating particles less than 100 microns in diameter since other methods, as described previously, are more convenient. Fine-mesh metal screens are available with pore sizes down to a few microns.

V. Conclusions

When the need arises to collect and move particles about on Earth, one ordinarily resorts to vacuum-cleaner-like devices for fine particles and scoops or shovels for large particles. Since an atmosphere exists on Mars, the problem of particle collection is similar to that on Earth, and one would conclude that pneumatic collection and transport methods would be most effective for fine particles. The vacuum necessary for pneumatic particle collection and transport can be produced by either an electrically-powered blower or a compressed-air aspirator pump.

Particle size fractionation can most easily be accomplished with a multi-stage impactor as described on page 13. Filtration can also be used for size fractionation; however, removal of the particles from the filter pores might be difficult.

A centrifuge could be used to fractionate particles on the basis of size and density. Centrifugation in a fluid of uniform density would be used to separate particles according to size. Further separations according to density could be obtained by means of density gradient centrifugation. The resulting size and density fractions could be individually studied for evidence of life.

BIBLIOGRAPHY

1. J. Stuart, Extraterrestrial Biological Instrumentation Problems, San Diego Symposium for Biomedical Engineering, 1963.

2. J. Lederberg and E. Levinthal, Cytochemical Studies of Planetary Microorganisms, Status Report covering period of March 1, 1962 - April 1, 1963.

3. A. R. Kriebel, Particle Trajectories in a Gas Centrifuge, Journal of Basic Engineering, September, 1961, 333.

4. A. J. Bolwell, Dust Sampler Uses Thermal Precipitation Principle, Design News, August, 1964.

5. Recommended Procedure for Aerosol Analysis, Millipore Filter Corporation, April 1, 1958.

6. R. C. Cadle, Particle Size Determination, Interscience, 1955.

7. C. P. Shillaber, Photomicrography in Theory and Practice, J. Wiley, 1947.

8. E. C. Levinthal, The Biological Exploration of Mars, Lecture 10, Horizons in Space Biosciences, University of California, April, 1964.

9. D. G. Rea, The Evidence For Life on Mars, Lecture 8, Horizons in Space Biosciences, University of California, April, 1964.

10. Study of a Manned Mars Excursion Module, Philco, Aeronautics Division, Publication No. C-2379, NASA Contract NAS9-1608, December 20, 1963.

11. Kent's Mechanical Engineers Handbook, Design and Production, Wiley, 1953.

12. Microscope System For Mars Study Program, Reports No. 2274, 2405, 2447, General Mills - Electronic Division, JPL Contract No. 950123, October, 1963.

13. Applied Science Division of Litton Industries, JPL Contract No. 950771, Monthly Progress Reports for January, February, March, April, May, 1964.

14. J. Lederberg and C. Sagan, Microenvironments for Life on Mars, Proceedings of National Academy of Sciences, Volume 48, No. 9, September, 1962.

15. G. Soffen, Limitations in Designing Life Detection Experiments, Symposium on Unmanned Exploration of the Solar System, American Astronautical Society, February, 1965.

16. G. Soffen, Experiments From Landers, Lecture 10, Horizons in Space Biosciences, University of California, May, 1964.

17. Millipore Corporation Data Manual, ADM-60, 1964.

PNEUMATIC SOIL SAMPLE COLLECTOR

Thomas W. Tourville
Research Assistant

Design Division
Department of Mechanical Engineering
Stanford University
Stanford, California

January 11, 1965

Supported by NASA under Contract No.NsG 81-60

OPERATION

The soil sample collector was designed to pick up particles of dirt from a flat surface and deliver them to the Multivator in the form of an aerosol. The collector uses compressed air and will collect only those particles smaller than 100 microns (.004 inches) in diameter when operated at an appropriate pressure.

Figure 1 shows the device in a cutaway view. The heart of the unit is the aspirator. The small tube in the center of the aspirator shoots a primary jet of high velocity air into the larger diameter outlet. Thus a low pressure zone is formed immediately behind the primary jet, and a secondary air stream is forced through the slots at the base of the aspirator. The three aerosolizer jets stir the dust particles through a spiraling path into the plastic funnel where they enter the secondary air stream of the aspirator. The air is supplied to the four jets by a circular pressure manifold in the aluminum base of the collector. The manifold is connected to the compressed air supply.

DESIGN

From information determined experimentally, the secondary flow rate was found to be approximately twice the primary flow rate at working pressures in the range 10-50 psi.

Since it was desirable to have the collector self-contained and independent of the outside atmosphere, the total flow rate of the three aerosolizer jets was set equal to the secondary flow rate of the aspirator. The problem therefore reduced to finding the correct inside diameter of the aerosolizer jets, given the diameters and lengths of the tubes making up the primary jet. This was accomplished by assuming that all flow resistances are due only to the internal resistance of the tubes, which were small enough in diameter to be considered as capillaries.

Following is the analytic solution to the above problem.

R_P = flow resistance of primary jet

$$R_P = \frac{\Delta P}{F_P}$$

where

ΔP = manifold pressure (gage)

F_P = primary flow rate

R_j = flow resistance of one aerosolizer jet

$$R_j = \frac{\Delta P}{F_j}$$

where

F_j = flow rate of one aerosolizer jet

F_S = secondary flow rate

$$F_S = 2F_P = 3\ F_j$$

$$\therefore\ F_j = 2/3\ F_P$$

$$\frac{\Delta P}{R_j} = 2/3\ \frac{\Delta P}{R_P}$$

$$F_j = 3/2\ R_P$$

D_P = inside diameter of primary tubes

D_P = .020 inches

L_P = total length of primary tubes

L_P = 1.6 inches

$$R_P = 1.0\ \frac{\text{lb.sec.}}{\text{in}^5}\ *$$

$$\therefore\ R_j = 1.5\ \frac{\text{lb.sec.}}{\text{in}^5}$$

*Gibson and Tuteur, Control System Components, p. 446, Fig. 12-10

L_j = length of one aerosolizer jet

L_j = .5 inches

D_j = inside diameter of an aerosolizer jet

$\therefore D_j$ = .015 inches

Aerosolizer tubes of the above diameter and length were cut from hypodermic needles and epoxied into holes in the aluminum base. They were bent 45° downward as well as 45° in a tangential direction in order to create a swirling action forcing the larger, unwanted particles to the side and the smaller particles up into the aspirator. Figure 2 is an assembly drawing of the collector showing dimensions and materials.

The collector was tested using samples of spherical glass beads of various diameters from 60 to 150 microns. A small sample of beads of a particular diameter was placed on a flat surface under the collector funnel. The pressure was increased slowly until the beads were seen to be ejected out the top. Figure 3 is a graph showing the manifold pressure required to pick up glass beads of a given diameter. The curve shows that if the operating manifold pressure is 38 psi, the cutoff point for glass beads will be 100 microns.

To check this result on dirt particles, various samples of soil were collected at the 38 psi operating point. The results showed that the 100 micron cutoff point was reasonably good for a wide variety of particles including gravel, black dirt, and chopped leaves.

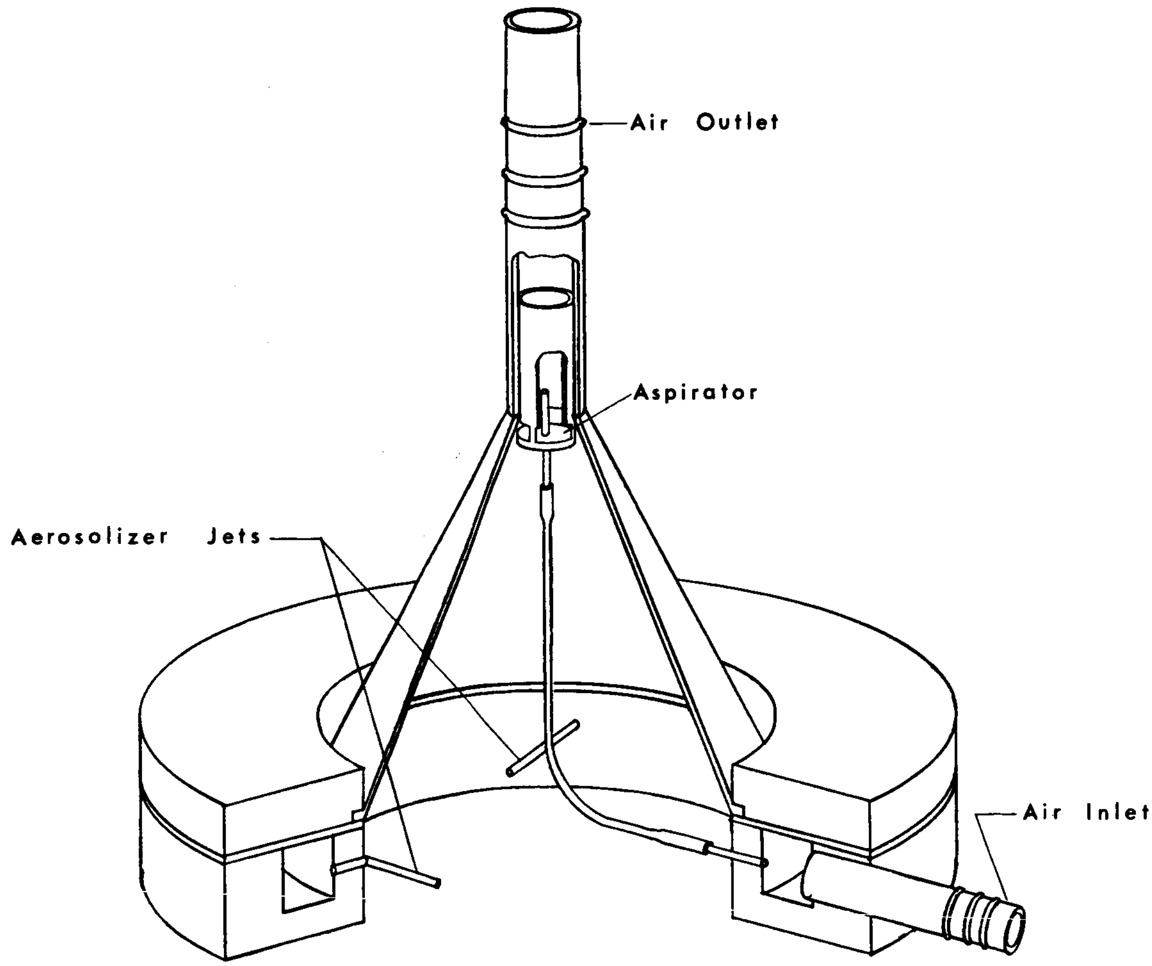

Soil Sample Collector

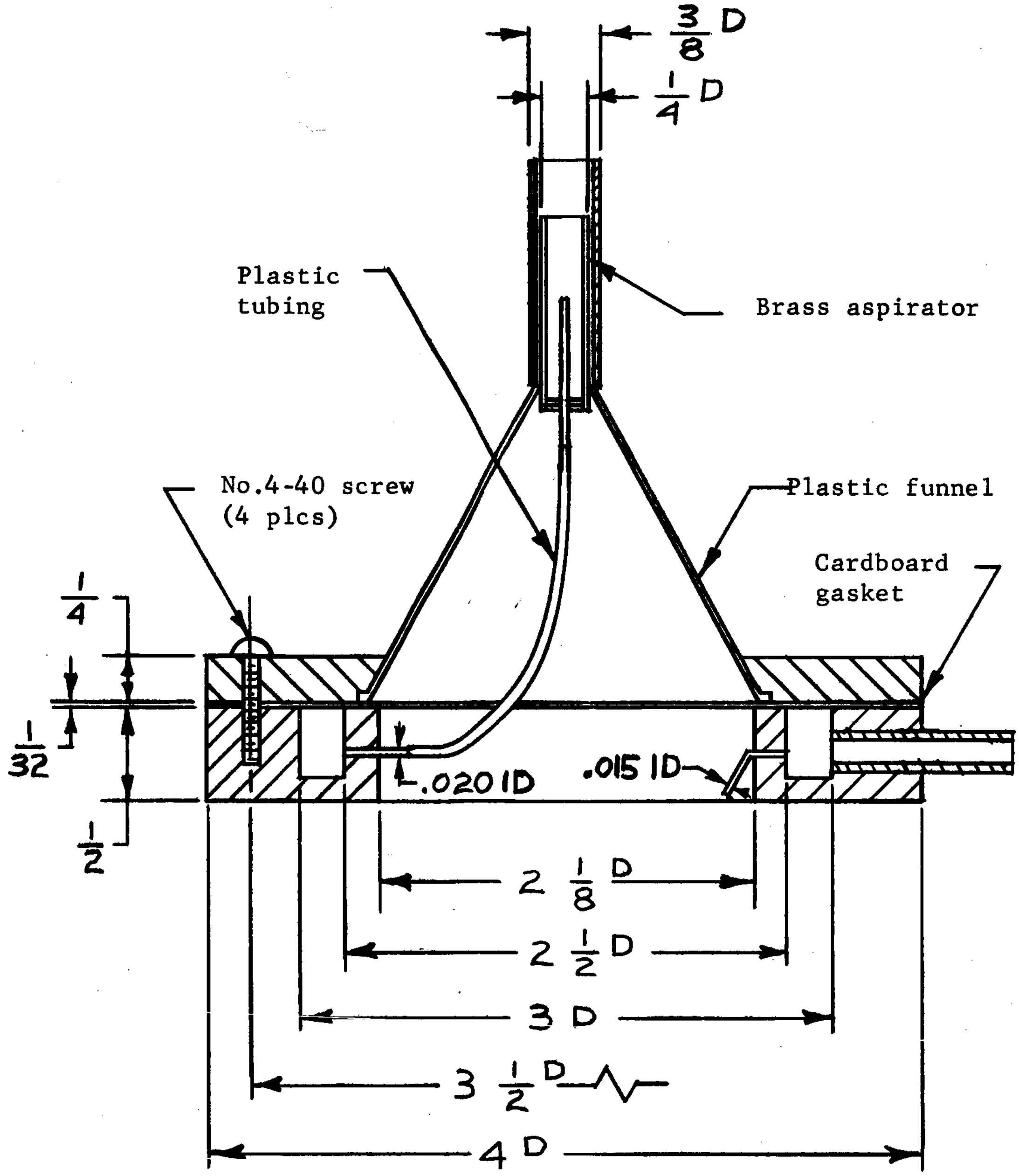

MATERIAL: Aluminum unless otherwise noted

TOLERANCES: ± 1/32

SCALE: Full

Figure 2

Diameter of spherical glass beads Vs.
Minimum manifold pressure required for collection

Figure 3

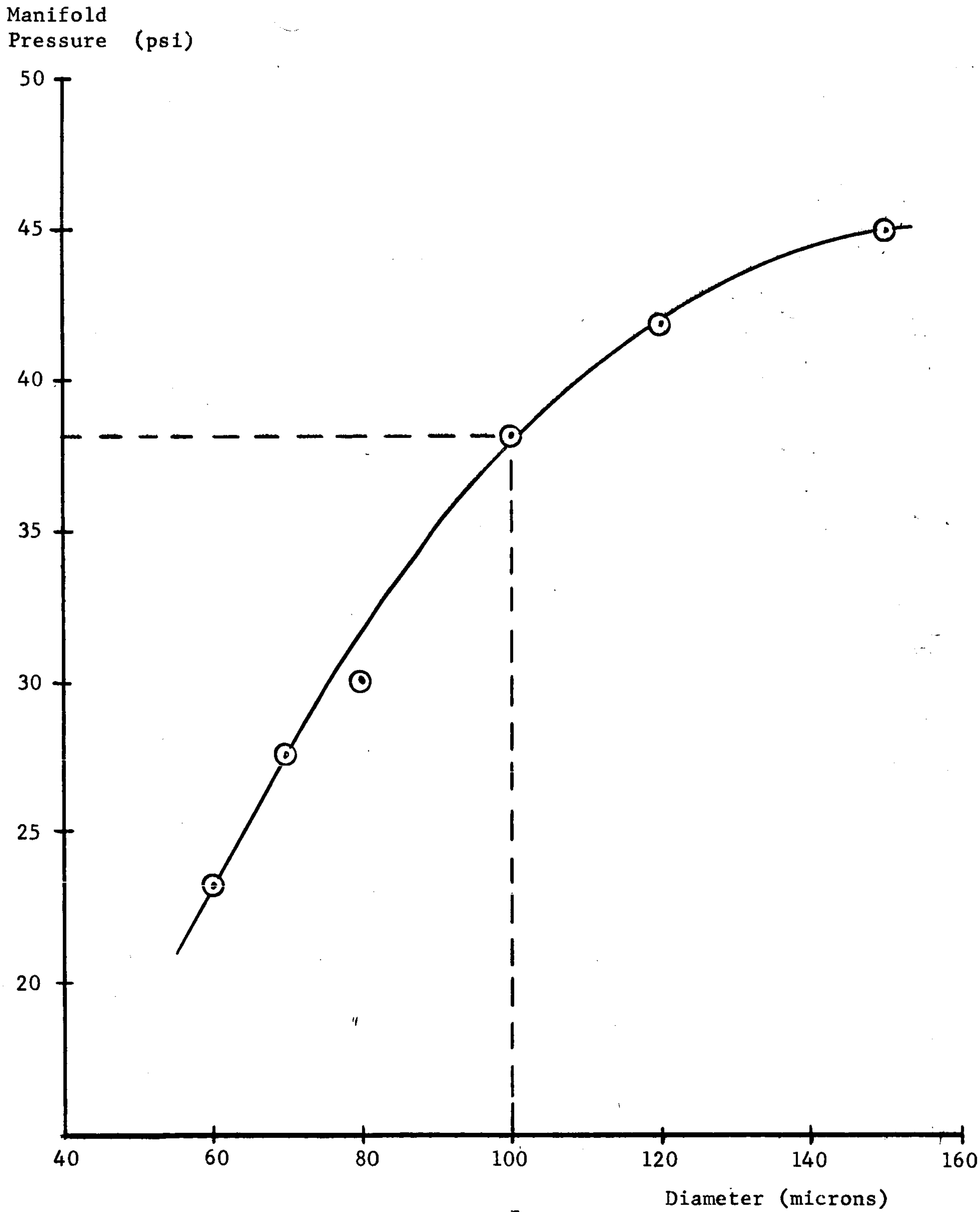

DELIVERING AND METERING MINUTE QUANTITIES OF A LIQUID

David S. Jacob
Research Assistant

William F. Lapson
Research Associate

Design Division
Department of Mechanical Engineering
Stanford University
Stanford, California

January, 1965

Supported by NASA under Contract No. NsG 81-60

Introduction

The object of this report is to discuss suitable methods for delivering and metering minute amounts of a given liquid which might be on the order of one microliter. The development of these techniques is important in certain aspects of biological research. As an example one might be interested in injecting a precise volume of a liquid chemical into the brain of an insect. Another example might be the delivery of a small finite volume of a reagent to see its effects on a single cell plant or animal.

The content of this report will be limited to the problem of titration wherein the delivered quantities of the liquid are minute and are capable of being measured to an order of accuracy of about one per cent of the delivered volume.

An attempt will be made to exercise the problem of titration by breaking the discussion into two categories, delivering and metering techniques.

Techniques of Delivery

We have observed that a liquid flowing slowly from the tip of an eye-dropper does not emerge as a continuous stream but as a succession of drops. A sewing needle, if placed carefully on a water surface, makes a small depression in the surface and rests there without sinking, even though its density is many times higher than that of water. When a clean glass tube of small bore is dipped into water, the water rises in the tube, but if the tube is dipped in mercury, the mercury is depressed. All these phenomena, and many others of a similar nature, are associated with the existence of a boundary surface between a liquid and some other substance. All surface phenomena indicate that the surface of a liquid can be considered to be in a state of stress, the material on one side of the line of contact exerts a pull on the material on the other side. This state of stress at the interface of two dissimilar materials is called surface tension.

In many engineering problems this surface phenomena is usually ignored since the magnitude of these forces is negligible relative to the other forces in a given system. For example the pouring of a large volume of water from a beaker (say 200 ml) can be precisely metered and delivered in a number of ways. There is usually a residue in the beaker due to the "wetting" action of the water on the surface of the bucket. However, the obvious affects of gravity completely dominate in this situation and the residue remaining in the beaker is negligible relative to the net delivered volume.

If we can imagine the beaker shrinking in size we see that the residue remaining after the liquid is poured becomes more and more a significant part of the total volume.

Capillarity

When a small bore glass tube is dipped into a container of water, the water will rise in the tube to a given height above the surface of the water in the container. On the other hand, if mercury is used instead of water it will be seen that the column will be depressed below the surface of the mercury. It can be shown that this phenomena is directly related to the effects of surface tension. A discussion of these relationships can be found in any number of physics textbooks and will not be developed here. However, the above phenomena of capillarity can be shown to follow the formula

$$y = \frac{2S\cos\theta}{\rho g r}$$

The terms are defined in the cgs system as:

y = height from surface of the liquid -cm

S = surface tension between the liquid and air (saturated with its own vapor) - dynes/cm

ρ = mass density of the liquid - gm/cm

r = radius of the capillary tube - cm

g = acceleration due to gravity - cm/sec^2

θ = contact angle between the liquid and the wall of the tube - degrees

In the above examples the angle of contact between water and the glass is less than 90° giving a positive value for y. And in the case of mercury the angle of contact is greater than 90° giving a negative value for y (see Figure 1). Obviously if $\theta = 90°$ then the height $y = 0$, i.e., no capillarity will exist.

If the liquid can be made to "wet" completely the interior of the tube its angle of contact with the wall is zero.

It can be shown that the meniscus is hemispherical and its radius is simply the radius r of the tube. The above formula does not take into account the height of the meniscus. If the height of the meniscus is not wholly negligible with respect to y then the mean value of y can be obtained by adding 1/3r to the height of the lowest point on the meniscus. The formula $y = \frac{2S\cos\theta}{\rho g r} + \frac{r}{3}$ is found to hold for tubes of as much as 1 mm diameter. For our purposes we shall confine ourselves to tubes of 1 mm or less in diameter.

Certain observations can be made about the surface tension S. Experiment shows that S almost invariably decreases with rise in temperature. The following formula for surface tension at temp t °C is found to hold well:

$$S_t = S_o(1 - \frac{t}{t_c})^n$$

where S_o is the value of S at 0°C

n is a constant which varies slightly from liquid to liquid but has a mean value of 1.2,

t_c the temperature where the surface tension between the liquid and its vapor is zero.

Figure 2 shows a plot of surface tension of water to air versus temperature.

<u>Micropipets</u>

Pipets of any size can be made simply by heating a glass tube under a flame of reasonably high temperature until the glass becomes soft and pliable. The tube is then withdrawn from the flame and is pulled at a constant rate. The tube will "neck" down to the approximate desired diameter at which the pulling motion ceases. In the case of micropipets it is desirable to perform the pulling or drawing operation in at least two successive stages. For example, if we begin with a tube of about

8 mm O.D. and 6 mm I.D. we may draw down to an O.D. of about 1 mm. After permitting the glass to cool, it may be heated again at approximately the center of the reduced section. The process of heating and drawing the glass tube is repeated once again except that a narrower flame must be used. The advantage of drawing in successive stages is that the amount of taper in the drawn portion is minimized. The final stage results in a tube having a bore ranging from 20 to 50 micrometers. It is usually not convenient to use pipets with smaller diameters since they are liable to become clogged. Micropipets may be categorized into two groups, those that depend for operation upon the strong surface tension at the tip, and those where the surface tension is eliminated from the bore of micropipet. The technique for eliminating surface tension will be discussed later.

For the first case it is found that the pressure inside the pipet is usually slightly higher than the atmospheric pressure, but the strong surface tension of the meniscus at the orifice prevents outflow of the working liquid into air. When this type of micropipet is adapted to a micrometer syringe, and with the air cushion in the pipet at a pressure higher than atmospheric, delivery is immediately obtained by immersing the tip into the experimental liquid in a watch glass or slide. In operating this type of micropipet the plunger of the syringe is depressed to a position where the liquid just begins to emanate from the tip of the micropipet. At this point the micropipet is carefully lowered into the liquid medium so that the liquid at the tip of the micropipet just touches the surface of the liquid medium. As the syringe is further depressed the liquid from the micropipet will be delivered in a continuous flow. The flow is stopped by withdrawing the tip from the liquid. In this manner the orifice at the tip acts like a stopcock for controlling the liquid flow. One advantage of this type of pipet is that, due to the strong forces at the meniscus, the working droplet remains at the tip without danger of outflow regardless of slight displacements of the plunger, which might accidentally occur. Of course the obvious disadvantage of this sort of system is that the experiment must be performed in a liquid medium and cannot be used effectively for delivery to a dry surface. Furthermore, precise quantitative deliveries are virtually impossible.

The other type of micropipet is one in which the surface tension is eliminated. The intent here is to improve the control of liquid flow from the pipet. The bore of the micropipet is made water repellent by treatment with Teddol, Akard, or paraffin wax. The effect of this treatment is to increase the contact angle to a value slightly greater or equal to 90 degrees. From the formula for capillarity $y = \frac{2S\cos\theta}{\rho g r}$ we see that y is zero or some small negative value when the contact angle $\theta = 90°$ or some value slightly greater than 90°.

Teddol and Desicote are commercial names of mixtures of volatile methyl chlorosilanes which may be used to eliminate surface tension. The tip of the clean and dry pipet is dipped in the liquid and suction is applied through the stem until the liquid fills the bore of the micropipet. After a few minutes the liquid is expelled. By this treatment the surface in contact with the liquid becomes water-repellent. Surface tension effects are almost completely eliminated, and the flow of liquid will depend almost entirely on the pressure applied by the micrometer plunger.

Methods similar to that described above are used when applying Akard or paraffin wax. In the case of paraffin wax the molten form is used. However, a serious disadvantage of wax coating is that a portion of it occasionally becomes detached and may get into the sample. For this reason, micropipets coated with paraffin wax are absolutely unsuited for gravimetric work.

Micropipets treated with these silicone water repellents (Teddol, Desicote) have several advantages. They are readily cleaned and dried since adhesion of aqueous solutions to the glass is greatly reduced by the repellent film. They also drain more completely than the uncoated pipets, and this minimizes the need for rinsing. If water-repellency is complete, micropipets deliver quantitatively the solution which they contain. This improves the precision of delivery of measured volumes since no residue is left which may be poorly reproducible. Complete water repellency produces a flat meniscus ($\theta = 90°$) which is more accurately read, improving the precision of calibrated micropipets. Furthermore, siliconizing the outside surface of the pipet inhibits the delivered liquid from creeping up on the outside of the tip.

Micrometer Syringe

A typical micrometer syringe is shown in Figure 3. It consists of a glass hypodermic syringe of a narrow uniform bore, attached to a micrometer screw. The glass syringe is held in a rigid framework and is secured in position by a collar. The plunger of the micrometer head presses directly on the piston of the syringe. The piston is spring-loaded by placing a weak spring constructed from piano wire around its stem so that the spring is held between the head of the piston and the lip of the syringe barrel. Spring loading in this fashion ensures that the piston may be advanced or retracted without lagging behind the corresponding movement of the micrometer plunger.

The micropipet is constructed in such a way as to be easily attached to the glass syringe by a simple rubber joint. In use, the syringe, the stem of the micropipet, and a part of the shank are completely filled with water. The rest of the shank contains an air cushion which serves to separate the water in the syringe from the sample or reagent solution in the tip or shaft of the micropipet. This air cushion transfers the pressure from the micrometer plunger via the piston of the syringe and the water column to the reagent solution in the shaft of the micropipet.

OUTLINE OF A PROGRAM FOR FUTURE STUDY

I. Survey of current literature
    A. Contact of manufacturers
        1. Reading of descriptive literature
            a. Techniques of glass working
            b. Various design approaches to automatic titration
II. Research of various textbooks
    A. Calibration methods
        1. Application of stereoscopic microscope
            a. Develop quantitative means of measuring volumes.
III. Set up elementary facilities
    A. Build a micrometer syringe
        1. Apply the syringe as a basic tool in metering quantitative amounts of a given liquid.
    B. Build glass drawing equipment
        1. Fabricate micropipets
    C. Build an automatically operated micrometer syringe
IV. Academic Studies
    A. Investigate surface tension phenomena
        1. Aqueous solutions
    B. Consult with various knowledgeable members of the faculty at Stanford

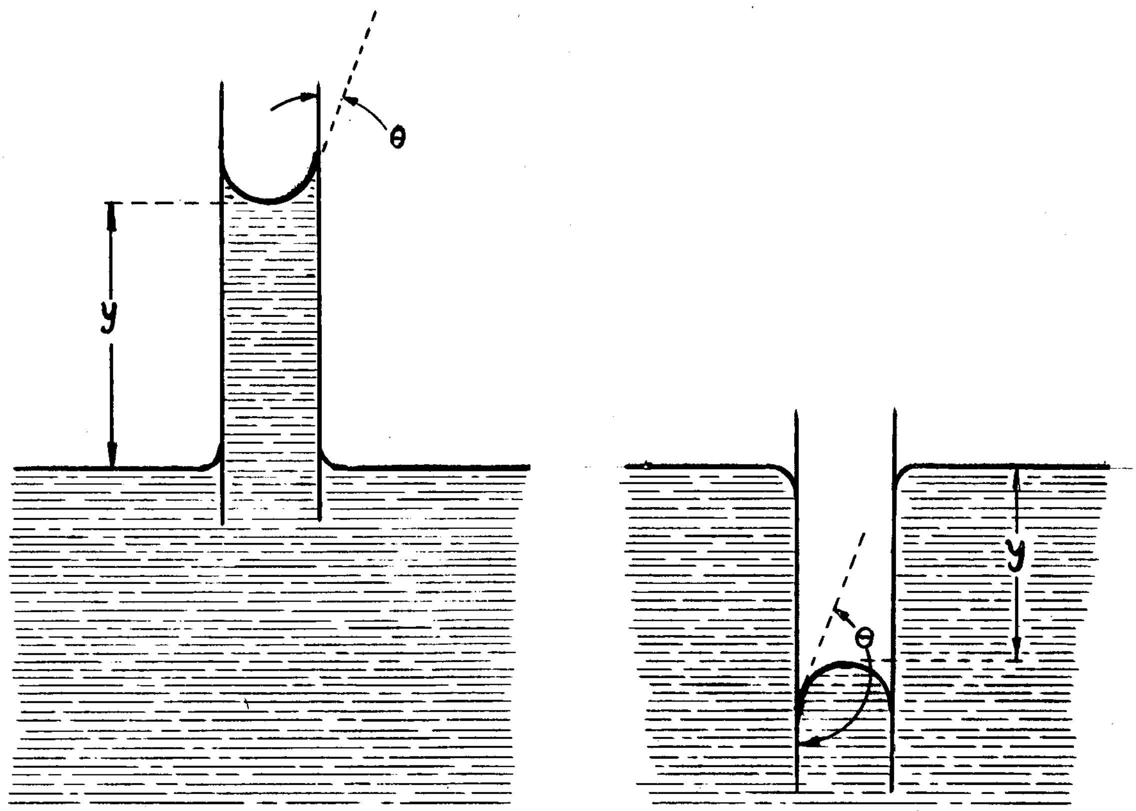

Figure 1

Surface Tension Forces on a Liquid in a Capillary Tube.
The liquid rises if $\theta < 90°$ and is depressed if $\theta > 90°$

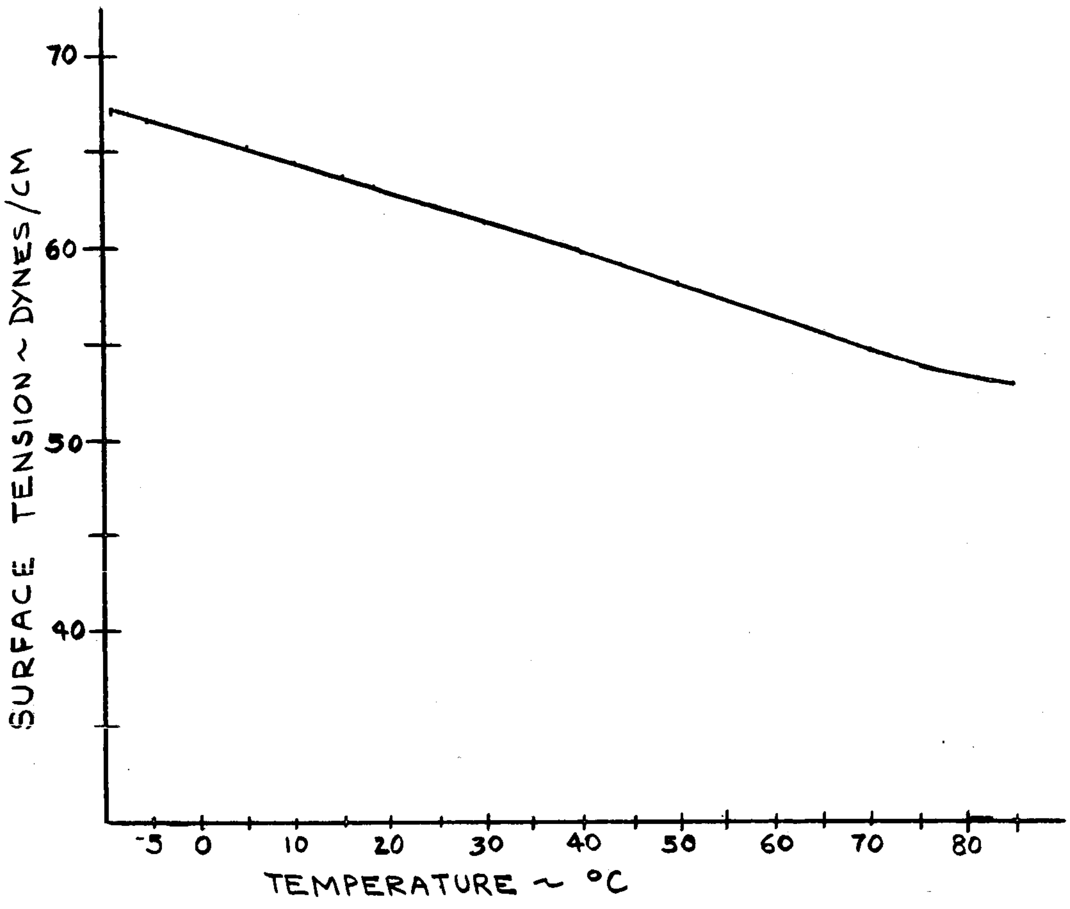

Figure 2

Plot of surface tension of water to air as temperature is varied

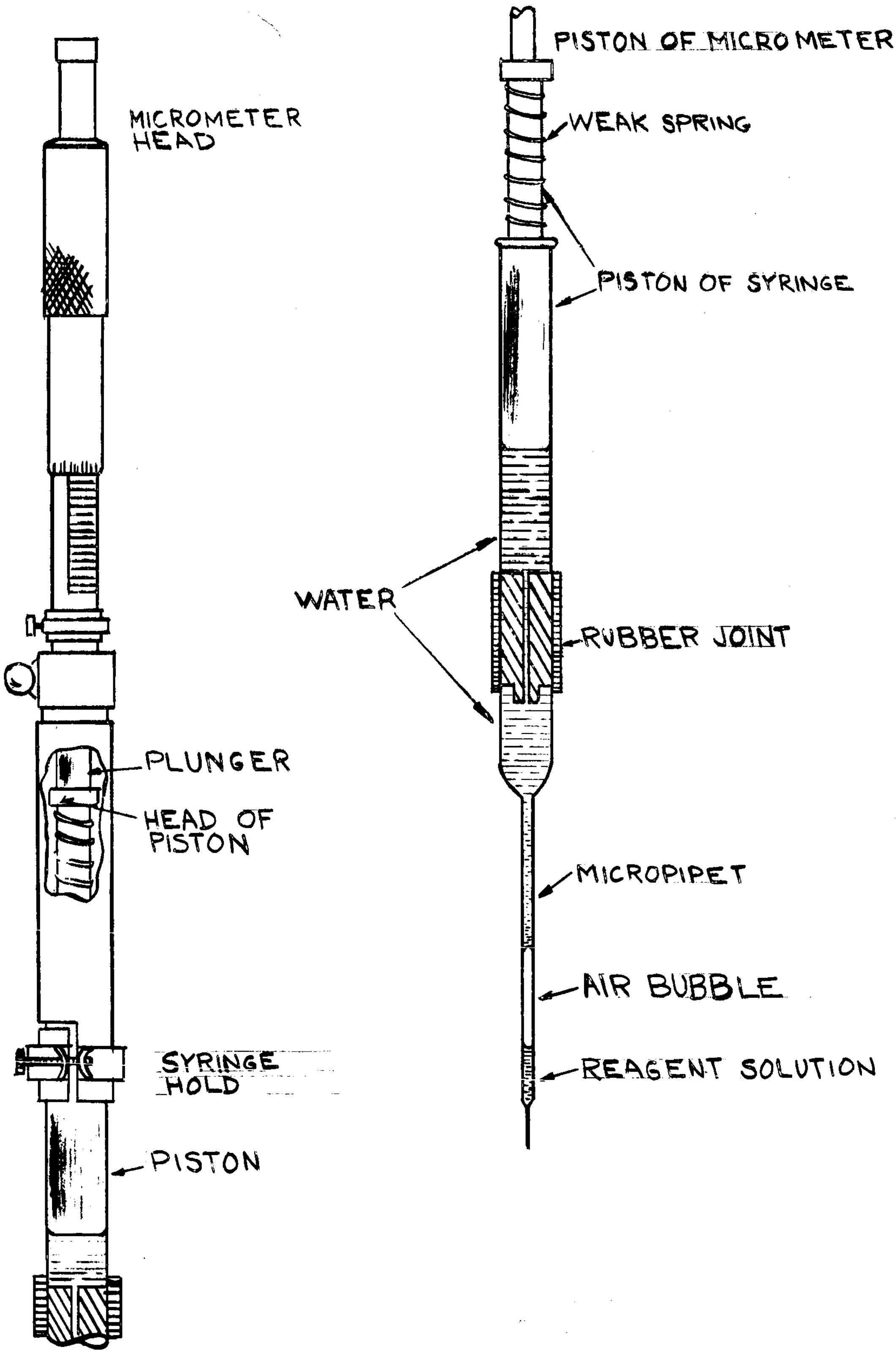

Figure 3. Micrometer Syringe and Micropipet

MINIATURE LINEAR DC SOLENOIDS

Thomas W. Tourville
Research Assistant

William F. Lapson
Research Associate

Design Division
Department of Mechanical Engineering
Stanford University
Stanford, California

October 6, 1964
Supported by NASA under Contract No. NSG 81-60

The purpose of this paper is to provide a means to compare miniature solenoids with other small, energy converting devices such as explosive, hydraulic, or pneumatic actuators. The material used in this paper was extracted from a catalog of solenoid components published by the Western Division of Imc Magnets Corporation.

The data on the following pages is restricted to linear DC solenoids weighing less than one pound. The maximum work done by a given solenoid was calculated by counting the squares under the force-displacement curve as given in the catalog. The curve representing the maximum rated voltage was used in all cases. The solenoid volumes listed are only approximate since they were calculated from the rough overall dimensions shown in the catalog.

The solenoids were divided into three classes: (I) single coil-pull-continuous operation; (II) single coil-pull-intermittent operation; and (III) single coil-push-continuous operation. The double coil solenoids were placed in the second classification since the coil used to do the work is operated intermittently while the additional coil only acts to hold the plunger at the end of the stroke. Page (5) is a summary of the data obtained for the three classes. Note that two different solenoids of a given weight may produce totally different amounts of work. This is due to variations in the shape of the plunger tip. Flat-faced plungers are used for relatively high forces at short strokes while conical-ended plungers are employed for a more constant force over a longer stroke.

Pages (6-10) are plots of various portions of the data given on page (4). The lines drawn on the graphs are meant to show only an <u>average</u> linear relationship between the ordinate and abscissa, and there is no intent to imply that the actual relationship should be linear. The results of these graphs can be summarized as follows:

(1) Average density of all solenoids: $3.3 \frac{\text{OZ}}{\text{IN}^3}$

(2) Average work done by class I solenoids (pull-continuous):

$$1.4 \frac{\text{IN-OZ}}{\text{OZ}}$$

(3) Average work done by class II solenoids (pull-intermittent):

$$4.5 \frac{\text{IN-OZ}}{\text{OZ}}$$

(4) Average work done by class III solenoids (push-continuous):

$$.62 \frac{\text{IN-OZ}}{\text{OZ}} \text{(up to weight of 8 oz.)}$$

$$1.4 \frac{\text{IN-OZ}}{\text{OZ}} \text{(above 8 oz.)}$$

The variation in the work done by push type solenoids is believed to be due to the fact that in small solenoids the hole in the stop or anvil is a relatively large fraction of the overall diameter of the plunger thus decreasing the number of flux lines acting between the anvil and the plunger. The work-to-power ratio is some indication of the efficiency of a solenoid, particularly in applications where response time is not critical. The plot of work-to-power ratio vs. weight for class I solenoids (page 7) shows that, in general, heavier solenoids are more efficient.

Note that all of the graphs show the maximum work that a particular solenoid will deliver. If the power input is decreased, the work output will decrease proportionately. If, however, the power input is increased so that the voltage is higher than the maximum rated figure, there may not be a continued increase in work output. This is because the iron becomes saturated with flux lines. This characteristic sets the practical limit on the maximum force available from a given solenoid. The formula for the force produced by a circular flat-faced plunger is:

$$F = \frac{B^2 r_1^2}{22.9} \; *$$

where

F is the force in pounds

B is the flux density in kilomaxwells per square inch

r_1 is the radius of the plunger

Using the best possible magnetic material with a maximum value

---

* Herbert C. Roters, Electromagnetic Devices, John Wiley and Sons Inc., 1941, p. 202, equation (8c).

for B of 15,000 gauss, the above equation becomes:

$$F_{max} = 101.5\ D^2 \quad (1b)$$

where D is the diameter of the plunger in inches. This equation is plotted on page (11) for easy reference.

There are four general conclusions which can be safely drawn from the above data:

(1) A solenoid designed for intermittent operation will produce about three times as much work as a solenoid of the same size and weight designed for continuous operation.

(2) Intermittent solenoids are less efficient than continuous ones.

(3) Very small push-type solenoids produce less work for their weight than do pull-types.

(4) Solenoids are limited to approximately one hundred pounds per square inch of the plunger's cross-sectional area due to saturation of the iron pole pieces.

NO.	TYPE	WT. (OZ)	VOLUME (IN^3)	DENSITY (OZ/IN^3)	MAX WORK (IN-OZ)	VOLTAGE	RESISTANCE	POWER (WATTS) (IN-OZ/WATT)	WORK/POWER	CLASS
4SD819-3	PULL-C	.071	.083	.856	.055	30	800	1.125	.049	
7SD822-1	PULL-C	.071	.262	.27	.896	30	53.4	14.6	.061	
5SD805-3	PULL-C	.635	.098	6.45	.155	28	218	3.6	.043	
5SD856-1	PULL-C	.640	.140	4.56	.367	28	234	3.35	.109	
8SD203-1	PULL-C	1.41	.367	3.84	.265	30	180	5.0	.053	
8SD203-3	PULL-C	1.41	.362	3.89	1.24	24	45	12.8	.097	
8SD328	PULL-C	1.81	.483	3.75	4.36	30	45	20.0	.218	I
9SD451-1	PULL-C	3.51	.900	3.90	5.2	24	24	24	.216	
10SD60-1	PULL-C	4.25	1.18	3.60	4.58	28	60	13.1	.350	
12SD128	PULL-C	4.75	1.50	3.17	5.78	28	53.4	14.6	.395	
13SD135-1	PULL-C	10.25	3.09	3.31	11.9	28	43.7	17.9	.665	
13SD136	PULL-C	10.25	3.09	3.31	17.1	28	43.7	17.9	.955	
				"C" - CONTINUOUS						
5SD960-3	PULL-I	.424	.11	3.85	1.75	30	32.6	24	.073	
7SD756-2	PULL-I	1.89	.342	5.53	3.73	28	30	26.1	.143	
8SD818-1	PULL-2	2.15	.631	3.40	8.7	30	4.8	187	.046	
8SD862-1	PULL-1	2.70	.597	4.54	15.7	30	4.62	195	.081	
10SD800-1	PULL-2	7.50	2.16	3.47	40.5	30	5.21	173	.235	II
13SD127-1	PULL-2	10.25	3.06	3.35	37.5	28	4.36	180	.209	
14SD47-1	PULL-2	11.25	4.46	2.53	30.5	28	6.0	131	.232	
13SD107-2	PULL-2	12.50	4.28	2.93	37.5	28	4.36	180	.209	
				"I" - INTERMITTENT "2" - 2 COIL						
9SD876-1	PUSH-C	2.33	.778	3.0	1.51	30	200	4.5	.336	
11SD772-5	PUSH-C	6.81	1.55	4.4	4.12	30	30	30.0	.137	
15SD72-1	PUSH-C	9.00	4.43	2.02	14.7	28	37	21.1	.697	III
17SD87-1	PUSH-C	12.00	5.70	2.10	18.5	28	30	26.1	.738	

EVALUATION OF THE HERCULES BA31K7 BELLOWS MOTOR USED IN THE MARK II MULTIVATOR

Prepared by Jack L. Harms, Research Assistant
Under Contract No. NASA 8160

August, 1964

Abstract

Tests were conducted on the BA31K7 bellows motor of Hercules Powder Company of the type incorporated in the current Multivator design. These tests showed that the bellows extended completely in 0.5 milliseconds or less but had an ignition delay time of 0.8 milliseconds. The rapid stroke gave rise to high accelerations on the order of 5000 g's which resulted in high inertial forces. The average work output was 36 in-lb over a 0.4 inch stroke, with initial starting forces of 160 lbs. Average stroke forces were computed to be 80 to 130 lbs. over the stroke length. The bellows motor received its power output from rapid heating and expansion of gases. The residual or holding force of the extended bellows was due to the rigidity of the casing, and was found to be about 2 1/2 times higher than the 20 lbs. noted by the manufacturer.

ACKNOWLEDGEMENTS

I wish to acknowledge the assistance of Bill Lapson in the collection of the data and the organization of this report. I would also like to acknowledge the assistance of Dan Rogers who helped design and construct the test apparatus.

Introduction

The tests described in this report were intended to provide insight into the performance of bellows motors of the type incorporated in the current Multivator design. The bellows motor used in these tests was motor No. BA31K7 of the Hercules Powder Company. The tests indicated how to interpret the manufacturer's specifications, and also allowed the energy output to be calculated. The manufacturer's specifications are given at the end of the report.

Summary of Test Results

The general test results revealed that the average delay time before bellows motion was 0.8 milliseconds at a firing current of 3 amperes. The actuation or stroke time was 0.6 milliseconds for resisting forces of 50 pounds or less and increased for increasing loads. This rapid stroke time caused large inertial forces which will probably be the major forces the designer will have to contend with in the motor's use. The motors get their power output from rapid gas heating and expansion; consequently, their stroke length and work output may be limited by a long stroke time. It is, therefore, recommended that these devices not be used for driving highly viscous loads which could result in long stroke times.

Tests showed that the bellows motor could deliver high initial starting forces of 160 pounds with average stroke forces of 82 to 127 pounds for an average stroke time of 0.6 milliseconds. For a longer stroke time of 1.1 milliseconds the average force was 42 to 66 pounds. The output force for this model bellows motor was rated by the manufacturer only by its holding force of 20 pounds for the rated 3/8 stroke length. The test results showed a maximum final holding force capability of about 47 pounds for a final stroke length of 0.38 to 0.42 inches. Consequently, the device has a safety factor of 2-1/2 with regard to the holding force. It should be noted that for loads above 50 pounds the final stroke length is unpredictable. With loads in excess of 50 pounds the bellows failed to extend to the rated 0.38 inches and after a few seconds collapsed to less than its initial fired length. The collapse was due to the cooling of the internal gases.

Description of Test Set-up

The physical test set-up shown in the figure on the following page consisted of a pressure tank to supply the load force, a piston and connecting rod to transmit the load to the bellows motor, a potentiometer and oscilloscope to measure and display the displacement-time curve, and a scope camera to record the results.

Apparatus Operation

The bellows motor was put into the firing chamber. Next the rod with the sliding contact of the potentiometer was placed in contact with the bellows motor. The rod was connected to the piston which moved in the cylinder in the pressure chamber. The oscilloscope was connected into the test circuit so that motion of the piston (and slider rod) caused a voltage displacement. The scope sweep was triggered by the firing circuit. Consequently, triggering the firing circuit triggered the sweep. This enabled us to obtain the delay time between initiation and incipient motion of the bellows motor. The piston displacement was assumed identical to the bellows motor's displacement. Consequently, the oscilloscope measured the bellows motor's displacement vs. time characteristics.

Test Procedure

First, the bellows motor was measured for its initial length. Then it was installed in the firing chamber. The pressure tank was pressurized to the test pressure causing the piston to push against the unfired motor. The motor was then removed and remeasured to detect any initial compression by the test force. After the motor was replaced, the zero line on the oscilloscope was set corresponding to zero displacement (the scale was adjusted so 0.1 inch displacement corresponded to 1 cm of the scope screen grid). Next, the pressure tank was repressurized to the test pressure and the scope camera was opened on "bulb" exposure. The firing circuit was closed and the bellows motor was fired, leaving its time-displacement trace recorded on the film. The fired bellows motor was then remeasured to detect any compression occurring outside the scope time range and to get an accurate final displacement. (Test Data recorded in laboratory notebook, pages 16 to 21.)

Test Results

The results of the several tests were for a constant firing current (2.8 amps) with load force a parameter. These tests yielded directly the time-displacement curves, the delay time, and the final displacement for a given loading force. The acceleration and velocity curves were derived by numerical differentiation of the displacement curves and thus are limited in their accuracy (estimated at ± 25%).

Estimate of Measurement and Calculation Errors

Micrometer reading of stroke	± 3%
Oscilloscope measurements	± 5%
Linearity of potentiometer	± 5%
Photograph readings (measurement of time and displacement)	± 8%
Calculation and round off error (Velocity, acceleration, parting position)	± 4%
Total Error	± 25%

Time	Test Number 3			Test Number 4			Test Number 5			Test Number 6		
illi- econds	acceleration inches/sec^2	inertial force (lbf)	output force (lbf)	acceleration inches/sec^2	inertial force (lbf)	output force (lbf)	acceleration inches/sec^2	inertial force (lbf)	output force (lbf)	acceleration inches/sec^2	inertial force (lbf)	output force (lbf)
to .8	0.0	0.0	0.0	0.0	0.0	0.0	0.0	0.0	0.0	0.0	0.0	0.0
.85	2×10^6	145	169	1.5×10^6	109	156	1.25×10^6	90.5	138	2×10^6	145	216
.95	10^6	72.4	96	0.0	0	47	5.0×10^5	36.2	83	0.0	0	71
1.05	10^6	72.4	96	1.7×10^6	123	170	1.75×10^6	127	174	1.6×10^6	116	187
1.15	10^6	72.4	96	6.0×10^5	43.5	91	3.0×10^6	217	264	-2.0×10^5	-145	-74
1.25	3×10^6	217	241	6.2×10^6	448	495	5.0×10^5	36.2	83	1.6×10^6	116	187
1.35	2.0×10^6	145	169	0.0	0	47	-1.0×10^6	-72,4	-25	0.0	0	71
1.45				-6.5×10^6	-478	-431	0.0	0	47	-1.0×10^6	-72.4	-2
1.55							5.0×10^6	-362	-315	-2.0×10^6	-145	-74
										0.0	0	71

Figure 6. Calculated Data, Acceleration Inertial Force, and Output Force vs. Time

TEST NO. 3		TEST NO. 4		TEST NO. 5		TEST NO. 6	
Displacement (inches)	Force Output (lbs)	Displacement (inches)	Force Output (lbs)	Displacement (inches)	Force Output (lbs)	Displacement (inches)	Force Output (lbs)
0.02	169	0.015	156	0.013	138	0.020	216
0.05	96	0.030	47	0.030	83	0.040	71
0.09	96	0.062	170	0.065	174	0.076	187
0.14	96	0.100	91	0.130	264	0.120	-74
0.22	241	0.200	495	0.200	83	0.170	187
		0.300	47	0.260	-25	0.220	71
0.32	169			0.320	47	0.260	-2
		0.335	-431			0.280	-74
				0.330	-315		
						0.300	71

Figure 7. Output Force vs. Displacement

Test No.	Resisting Force (Lbf)	Separation Point	% of Max. Bellows Motor Displacement before Separation
3	24	0.26 inches	62%
4	47	0.36 inches	95%
5	47	0.36 inches	90%
6	71	0.28 inches	97%

Figure 8. Calculated Piston Separation Points

	Test No. 3 30 psi	Test No. 4 60 psi	Test No. 5 60 psi	Test No. 6 90 psi
Maximum Initial Stroke (inches)	0.42	0.38	0.40	0.39
Average Output Force over Stroke (lbs)	145	83	56.4	72.5
Average Total Work Output (in-lbs)	61.0	31.4	22.5	28.3

Figure 9. Average Total Work Output

Significance of Test Results

The tests showed that the tested bellows motors were conservatively rated with regard to holding force and stroke length. Actual holding forces shown in Fig. 5 were found to be as high as 47 pounds for the rated stroke. The results confirmed the manufacturer's specifications regarding actuation time of 0.5 milliseconds. However, the test also revealed an 0.8 millisecond delay time before actuation. It should be noted that large, inertial forces were created due to the extremely fast actuation time. (These forces, given in Figure 6, were the dominant load forces graphed in Figure 4.)

The displacement-time curves show an almost linear displacement for the first two milliseconds. Consequently, the device's velocity can be assumed constant with good accuracy. Using this assumption the separation point given in Figure 8 of the piston shaft from the bellows motor was calculated, and data after this point was not used for force calculations. The final stroke displacement (Figure 5) varied directly with the resisting load for loads above 50 pounds but was uniformly constant for any load from 0 to 50 pounds. The work output (Figure 9) was approximately constant over the range of loads tested with the average output of 36 in-lbs. for a 0.40 inch stroke. This output compared to 8 in-lbs, if the holding force is assumed to be the average stroke output force, means that the designer can expect at least double the work output calculated from the manufacturer's holding force data and still be safe.

One interesting test result was the fact that the bellows motor obtained its force output from rapid heating of gases inside it rather than through gas generation. This was verified in tests with loads over 50 pounds in which the gases had cooled enough after 50 milliseconds to allow crumpling of the extended bellows by the load. Consequently, the usable force output and maximum stroke length are governed by the speed of the stroke. For a very viscous loading of equivalent resisting force one should expect a reduction in the stroke of the bellows motor, due to the reduction in the stroke velocity. Thus, the resulting longer stroke time would allow more energy to be lost through cooling. For space applications where the environment is apt to be something less than room temperature this device will deliver more of its available work output out as heat and thus lessen its terminal stroke length (assuming viscous loading). The residual holding force by which the company rates this particular bellows motor was found to be due to the rigidity of the bellows casting. Tests conducted with an expanded bellows motor with and without a hole in the case showed that the residual internal pressure is negligible in producing the residual force. One test showed that sufficient heat transfer had occurred to allow crumpling from the pressure load after 50 milliseconds.

General Conclusions

The test results were somewhat limited in their accuracy due to the fact that sliding friction of the system was unaccounted for and the data was only valid up to the point where the piston and shaft separated from the expanding bellows motor. These errors were considered small due to the large size of the resisting force compared to an estimated friction force of less than one pound. This force was assumed due to friction of the bellows motor moving along the sides of the firing chamber. Also the separation point occurred after at least 60% of the bellows motor's maximum extension. The major item which interferred with the quality of the tests was the actual data recording on film. This data was hard to read accurately due to the quality of the picture and the thickness of the oscilloscope trace. It probably could be recorded better if a Sanborn fast response recorder were used instead of the oscilloscope and camera.

Other improvements which could be made to the test set-up would be a pressure transducer which could plug into one of the Sanborn's recording channels. This pressure transducer in the pressure tank could detect if the tank pressure did stay constant as assumed or whether the rapid piston motion caused shock waves in the chamber. These shock waves might account for the buffeting actions observed in the acceleration and velocity of the piston. Another improvement to the set-up would be an adjustable firing chamber which would fit more closely around the bellows motor. With a close-fitting sleeve, the bellows motor may be able to deliver more force and more work before crumpling. Also some kind of adjustable detent is needed to keep the piston from crushing the bellows motor before firing. By having it adjustable the piston and bellows motor could be brought into contact. Then the bellows motor would immediately be opposed by the resisting load when fired.

Consideration of the bellows motor as a mechanical actuator showed that it is a very efficient device. When the bellows motor was compared with a theoretical helical spring of the same size, it produced better than ten times the work output per unit weight than the spring. Even using the rated holding force in the calculation of the work output, the bellows motor was several times better. Further comparisons of the bellows motor and a solid bar spring showed that the bellows motor produced more than ten times the energy per unit weight than stored in the solid bar. A final comparison of the specific energy output of the bellows motor to that of gunpowder or hydrazine shows that its output is about one thousandth of that which could be delivered by and equivalent weight of pure explosive charge. Consequently, though the present bellows motor has a high energy-to-weight ratio, it is theoretically possible to improve the device to deliver even more energy.

Comparison of the Specific Work of the Hercules BA31K7 Bellows Motor and a Theoretical Helical Spring

Specific Work Output of the Bellows Motor

Average work output = 36 in-lb for a 0.40 inch stroke

Dimensions (unfired):

Diameter: 0.320 inches

Length: 0.625 inches

Bellows motor's weight = 2.185 gms = 4.83×10^{-3} lb.

W_s, specific work output = $\frac{36 \text{ in - lbf}}{4.83 \times 10^{-3} \text{ lbm}}$

$W_s = 7450$ in - lbf/lbm

Using the rated holding force of 20 lbs:

W_s, average work output = 8 in - lbf for a 0.40 inch stroke

$W_s = 1660$ in - lbf/lbm

Helical Spring Specific Work Output

For an ideal helical spring (of the same size as the bellows motor)

$$\tau \max = \frac{16 \, PR}{\pi d^3} \left(1 + \frac{d}{4R}\right) \quad * \qquad 10)$$

P = load applied to spring

R = the outside radius of the spring

d = the thickness of the spring coil

δ = the stroke length for the spring

R = 0.16 inches (the radius of the bellows motor)

τmax = the maximum shear stress in the spring

Assuming steel (oil quenched 0.8% carbon)

ρ, the density, = 0.283 lb/in^3

The proportional limit, τ = 96,000 psi

Shear Modulus of Elasticity G = 12×10^6 psi

* Timoshenko and Young, Elements of Strength of Materials, 4th edition. D. Van Nostrand Co. Inc. 1962, p. 78.

Let τmax = τ proportional limit for maximum work storage.

Solving formula 10 for P

$$P = \frac{\tau max.\pi d^3}{16R\ (1 + \frac{d}{4R})} \qquad (11)$$

For a helical, closely coiled spring: (12)

$$\delta = \frac{64nPR^3}{d^4G} \ *$$

where

n = the number of spring coils

G = the shear modulus of elasticity

Solving for the spring constant, K, substituting for P, S from equations (11) and (12):

$$K = \frac{P}{\delta} = \frac{\tau max.\pi d^3}{16R\ (1 + \frac{d}{4R})} \quad \frac{d^4G}{64nPR^3}$$

$$K = \frac{\pi\tau max.d^7G}{16(64)R^4n(1 + \frac{d}{4R})} \quad \frac{16R(1 + \frac{d}{4R})}{\tau max.\pi d^3} \qquad (13)$$

$$K = \frac{Gd^4}{64R^3n}$$

Substituting for P in equation 12 and solving for δ in terms of $\tau max.$:

$$\delta = \frac{64nR^3}{Gd^4} \quad \frac{\tau max.\pi d^3}{16R(1 + \frac{d}{4R})}$$

$$\delta = \frac{4\pi R^2 n\tau max.}{Gd(1 + \frac{d}{4R})} \qquad (14)$$

---

* Timoshenko and Young, Elements of Strength of Materials, 4th Edition. D. Van Nostrand Inc., 1962, p. 78.

Using formulas (13) and (14) to solve for total work output of a spring:

$$\text{Work} = \frac{1K\delta^2}{2}$$

$$= \frac{1}{2}\frac{Gd^4}{64R^3n}\left(\frac{4\pi R^2 n\tau\text{max.}}{Gd(1 + \frac{d}{4R})}\right)^2$$

$$= \frac{1}{2}\frac{Gd^4}{64R^3n}\;\frac{16\pi^2R^4n^2\tau\text{max.}^2}{G^2d^2(1 + \frac{d}{4R})^2}$$

$$\text{Work} = \frac{1}{2}\frac{\pi^2Rd^2n(\tau\text{max})^2}{4G(1 + \frac{d}{4R})^2} \qquad (15)$$

Assuming the spring will occupy the same volume as the unfired bellows motor when the spring is fully compressed.

$$n = \frac{0.625}{d}$$

Let $d \rightarrow R = 0.16$

$n = 3.9$ coils $= 4$

$$\text{Maximum work output} = \frac{1}{2}\;\frac{\pi^2(.16)^3 4(96{,}000)^2}{4(12 \times 10^6)\;(1.25)^2}$$

Maximum work = 9.94 in-lb. for a spring stroke of

$\delta = .0515$ inches

Spring weight $= 0.283\ \text{lb}/_{\text{in}^3}\ \pi R^2(n)(d)$

$$= 1.42 \times 10^{-2}\ \text{lb}$$

the maximum specific work is given by:

W_s, specific work $= \dfrac{\cancel{9.94\ \text{in-lb}}}{1.42 \times 10^{-2}\ \text{lb}} = \dfrac{\cancel{700}\ \text{in-lb}}{\text{lb. of steel}}$ for a .0515 inch stroke.

For a more realistic spring let d be such that $\delta = 0.40$ inches, the stroke of the bellows motor.

From equation (14)

$$\delta = \frac{4\,R^2 n \max.}{Gd\left(1 + \frac{d}{4R}\right)} \quad \text{and } n = \frac{\text{compressed spring length}}{\text{coil diameter}} = \frac{0.625}{d}$$

substituting for n and solving the above equation for d:

$$d^3 + 4Rd^2 - \frac{16\,R^3(.625)\max}{\delta G} = 0$$

substituting in known values:

$$d^3 + .64d^2 - 2.58 \times 10^{-4} = 0$$

$$d = .02 \text{ inches}$$

Solving for the work output using equation (15):

$$\text{Work} = \frac{1}{2}\,\frac{^2(.16)(.02)^2\left(\frac{.625}{.02}\right)(96{,}000)^2}{4(12 \times 10^6)\left(1 + \frac{.02}{4(.16)}\right)^2}$$

Total work = 1.84 in-lb for

$\delta = 0.40$ inches

$$\text{Weight of spring} = 0.283\ \text{lb}/_{\text{in}^3}\left(R^2 - (R-d)^2\right) nd$$

$$= 0.283\ \text{lb}/_{\text{in}^3}\ (.625)\ (.16^2 - .14^2)$$

$$= (0.283\ \text{lb}/_{\text{in}^3})(.625)\ (.006)\text{in}^3$$

$$= 3.34 \times 10^{-3}\ \text{lb}$$

Specific work output:

$$\frac{\text{Total work}}{\text{Spring weight}} = \frac{1.84\ \text{in-lb}}{3.34 \times 10^{-3}\,\text{lbm}} = \frac{550\ \text{in-lb}}{\text{lbm}}$$

$$\text{Specific work output} = \frac{550\ \text{in-lb}}{\text{lbm}}$$

for a stroke of 0.40 inches (the stroke of the tested bellows motor)

Further idealization resulted in calculation of the energy storage capacities of a solid steel bar in pure compression and of a pure explosive charge.

Specific Energy of Solid Spring (Solid Bar)

$$U = \frac{P\delta}{2} \tag{16}$$

where U = strain energy (in-lb)

P = load (lb)

δ = the deflection due to the load (inches)

$$P = \sigma A \tag{17}$$

where A = the area of the bar

σ = the tensile stress

l = the length of the bar

Using Hooke's Law:

$$\delta = \frac{Pl}{AE} \tag{18}$$

where E = the modulus of Elasticity

Therefore, substituting for P and δ using equations (17), (18):

$$U = \frac{\sigma^2 Al}{2E} \tag{19}$$

Using steel (oil quenched 0.8% carbon)

$E = 30 \times 10^6$ psi

$\sigma = 120{,}000$ psi

$p = 0.283\ \text{lb}/_{\text{in}^3}$

$$U = \frac{144 \times 10^8 Al}{60 \times 10^6}$$

Volume = $A\ell = (.625)\dfrac{(.32)^2\pi}{4}$ (using volume of unfired bellows motor)

Volume = 5.03×10^{-2} cubic inches

Weight = $0.283 \times 5.03 \times 10^{-2} = 1.42 \times 10^{-2}$ lb

Therefore the maximum specific strain energy stored by weight:

$$U_s = \frac{144 \times 10^8 Al}{60 \times 10^6 (Al\rho)} = 850\ \text{in-lb}/_{\text{lbm}}$$

The Specific Energy Output of Gunpowder and Hydrazine

For normal gunpowder:

E_s, the specific energy output = 740 cal/gm

1 lb = 454 gm

1 cal = 3.087 ft-lb

= 37.1 in-lb

Using the conversion factors:

$$E_s \text{ (gunpowder)} = (740 \text{ cal})454 \text{ gm}/_{\text{lbm}} \frac{(37.1 \text{ in-lb})}{\text{cal}}$$

$$E_s = 1.25 \times 10^7 \text{ in-lb}/_{\text{lbm}}$$

For hydrazine (N_2H_4):

E_s, the specific energy output = 38.1 Kcal/$_{\text{mole}}$

1 mole = 32 gms

1 Kcal = 37.1×10^3 in-lb

Using conversion factors

$$E_s = \frac{38.1 \text{ Kcal}}{32 \text{ gm}} \times \frac{454 \text{ gm}}{\text{lbm}} \times 37.1 \times 10^3 \text{ in-lb}/_{\text{Kcal}}$$

$$= 2.01 \times 10^7 \text{ in-lb}/_{\text{lbm}}$$

SAMPLE CALCULATIONS

The purpose of this section is to demonstrate the methods used in reducing the test data to the previous tabulated form.

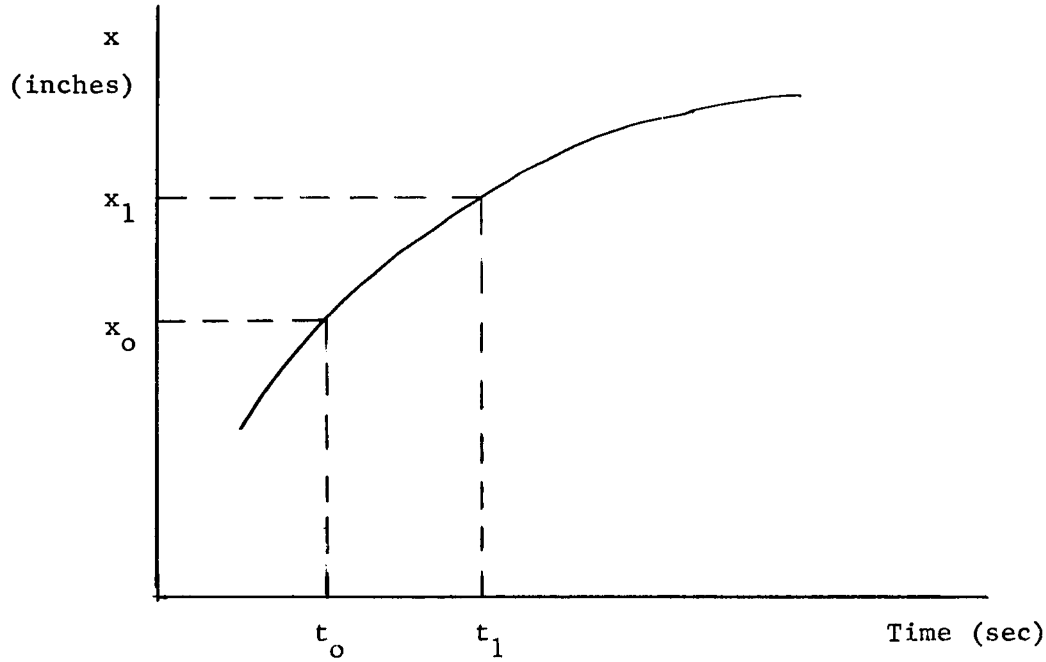

Figure 10 - Displacement - Time Curve

Velocity Calculations

From basic calculus:

$$v = \frac{dx}{dt} \quad \text{for linear motion} \tag{1}$$

Using the numerical approximation:

$$v = \frac{\Delta x}{\Delta t} = \frac{x_1 - x_o}{t_1 - t_o} \tag{2}$$

From the raw test data, test no. 3, page 25 of Project Multivator laboratory notebook no. 3:

t_o = .8 milliseconds $\qquad x_o$ = 0 inches

t_1 = .9 milliseconds $\qquad x_1$ = 0.02 inches

$$v_1 = \frac{x_1 - x_o}{t_1 - t_o} = \frac{(.02 - 0)\ \text{inches}}{(.9 - .8) \times 10^3\ \text{sec.}}$$

$$v_1 = \frac{.02\ \text{inches}}{10^{-4}\ \text{seconds}} = 200\ \text{inches/second}$$

at $t_1 = 0.9$ milliseconds

However, since this velocity is assured constant over the 0.1 millisecond time interval, t average = 0.85 milliseconds was used for graphs and tables.

Acceleration Calculations

From calculus:

$$a_1 = \frac{d^2 x_1}{dt^2} = \frac{dv_1}{dt_1} = \frac{\frac{dx_1}{dt_1} - \frac{dx_1}{dt_1}}{dt_1} \qquad (3)$$

Using the numerical approximation:

$$a_1 = \frac{\frac{\Delta x_1}{\Delta x_1} - \frac{\Delta x_0}{\Delta t_0}}{\Delta t_1} = \frac{\frac{x_1 - x_0}{t_1 - t_0} - \frac{x_0 - x_{-1}}{t_0 - t_{-1}}}{t_1 - t_0}$$

$$a_1 = \frac{x_1 - x_0}{(t_1 - t_0)^2} - \frac{x_0 - x_{-1}}{(t_0 - t_{-1})(t_1 - t_0)} \qquad (4)$$

From test data, test no. 3, page 25 of notebook no. 3:

$x_1 = .02$ inches $\qquad t_1 = 0.9$ milliseconds

$x_0 = 0$ inches $\qquad t_0 = 0.8$ milliseconds

$x_{-1} = 0$ inches $\qquad t_{-1} = 0.7$ milliseconds

$$a_1 = \frac{(.02 - 0) \text{ inches}}{(10^{-4} \text{ sec.})^2} - 0$$

$$= 2 \times 10^6 \text{ inches/(second)}^2$$

Force Calculations

Resisting Pressure Force (Load):

This force was considered constant due to the large tank volume compared with the volume displaced by the piston motion.

Piston Area: A_p: 0.785 square inches

Pressure Force, F_p: tank pressure x piston area

$$F_p = P \times A_p \tag{5}$$

e.g., at 60 psi tank pressure

F_p = 60 psi x 0.785 square inches

= 47.1 pounds force

Inertial Forces

Inertial forces are the forces associated with a mass under acceleration. In this experiment, these were quite large and very important.

Inertial force, $F_1(t) = M \times A(t)$ (6)

where

M = the mass of the moving system, is the piston, shaft, etc. The mass associated with the moving part of the bellows was neglected.

A(t) = the system's acceleration, inches per square second, at some time, t.

From measured data:

M = .0279 pounds weight (a weighed quantity)

The gravitational constant, $g = 386 \frac{\text{inches}}{\text{sec}^2}$

$$M = \frac{.0279}{386} = 0.724 \times 10^{-4} \frac{\text{lbs. - sec.}^2}{\text{inches}}$$

From reduced data of test no. 3:

at $t = t_2 = 1.0$ milliseconds

$$a(t_2) = 10^6 \text{ inches/sec}^2$$

$$F_1 \ (t_2) = 0.724 \times 10^{-4} \ \frac{\text{lbf - sec.}^2}{\text{inches}} \times \frac{10^6 \text{ inches}}{\text{sec.}^2}$$

$$= 72.4 \text{ lbf.}$$

Bellows Motor Output Force Calculation

The bellows motor force output $F_B(t)$ equals the sum of the opposing forces at any time, t. Referring to the diagram:

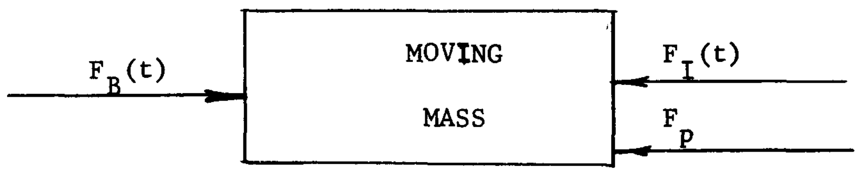

Figure 11 - Force Diagram

$$F_B(t) = F_p + F_I(t) \tag{7}$$

Neglecting viscous effects as being very small.

Using previous test data from test no. 3

at $t = t_2 = 1.0$ milliseconds

$F_p = 23.6$ lbf.

$F_I(t_2) = 72.4$ lbf.

$$F_B(t_2) = 72.4 + 23.6 = 96.0 \text{ lbf.}$$

Total Work Output

With the calculation of the output force vs. time, and using the displacement vs. time characteristics,to relate the force with displacement the output force vs. displacement curve was constructed. Then the average force output* over the total displacement, the average work was computed:

Average Total Work Output = Average Force Output x Stroke Length

$$W_T = F_A \times d \quad (8)$$

Calculation of Piston Separation

From the examination of the displacement time curves, it was noticed that the piston of the test set-up seemed to separate from the bellows motor. This resulted in the observed overshoot. Consequently, any results after separation would not be useful, because they would describe the piston and shaft's motion but not necessarily that of the bellows motor.

To calculate the point of separation the following assumptions were used:

1. The sliding friction and viscosity forces were negligible.
2. The tank pressure force was constant.
3. The velocity was constant over the interval before separation.

Under the above assumptions the change in kinetic energy of the moving system (i.e., the piston, shaft, etc.) will equal the work done by moving the system over the overshoot displacement against a constant load.

$$1/2\ MV_1^2 - MV_2^2 = F_p(x_f - x_s) \quad (9)$$

$V_2 = 0$ at max. overshoot displacement

The formula reduces to

$$1/2\ MV_1^2 = F_p(x_f - x_s)$$

---

* The average force output equals the sum of the forces over their stroke divided by the number of forces summed, i.e., for test no. 3 table no. 2

$$\text{Favg.} = \frac{169 + 3(96) + 241 + 169}{6} = 145 \text{ lbf.}$$

where

V_1 = the average velocity of the piston over the time to maximum displacement

M = the mass of the moving system

F_p = the resisting pressure force

x_f = the maximum displacement

x_s = the point where separation occurs

For test no. 3

$$V_1 = \frac{.67 \text{ inches}}{1.2 \text{ milliseconds}} = 558 \text{ inches/second}$$

$$M = 0.724 \times 10^{-4} \ \frac{\text{lbs-sec}^2}{\text{inch}}$$

$$F_p = 30 \text{ psi} \times .785 = 23.6 \text{ lbs.}$$

$$x_f = 0.74 \text{ inches}$$

$$x_s = .74 - \frac{(.724 \times 10^{-4})(558)^2}{2(23.6)}$$

$$x_s = 0.74 - .48 = 0.26 \text{ inches}$$

System Friction Forces

The moving system had negligible friction associated with it. Consequently, the remaining friction in the system was that of the bellows motor rubbing along the wall of the firing chamber.

Assuming:

1. a friction coefficient μ of 0.3 for Aluminum
2. a constant force throughout the stroke of 100 lbs.

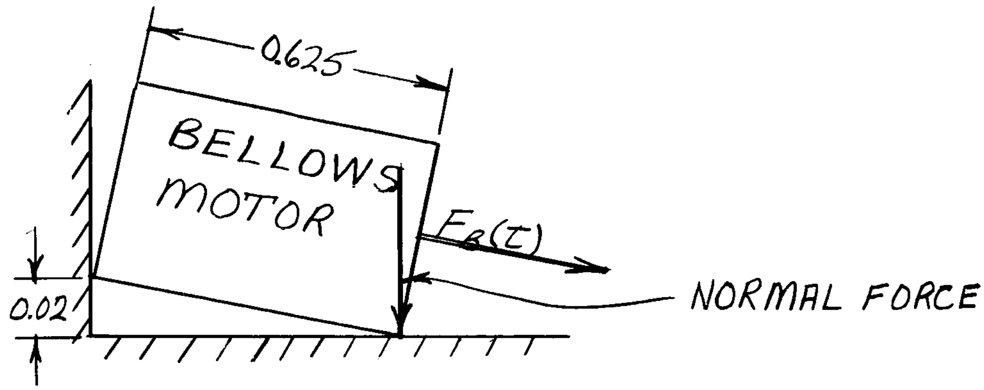

Figure 12 - Friction Force Diagram

$$\text{Normal Force} = 100 \text{ lbs } \frac{0.02}{.625}$$

$$= \frac{2}{.625} = 3.2 \text{ lbs.}$$

$$\text{Friction Force} = \mu \times \text{normal force}$$

$$= 0.3 \times 3.2 = 0.96 \text{ lbs.}$$

FEASIBILITY STUDY OF SPUR GEAR TRAIN FOR OPERATING A ROTARY VALVE.

BY: TAK OKABE

SOME PEOPLE IN DESIGN DIVISION AT STANFORD ARE ENGAGED IN A PROGRAM OF LIFE DETECTION OF MARS. THIS ROTARY VALVE WHICH IS DISCUSSED IN THIS PAPER IS A PART OF MECHANISM WHICH WILL BE USED FOR THE PURPOSE.

THE ROTARY VALVE, WHICH HAS EIGHT DIFFERENT CHANNELS, IS TO BE OPERATED BY AN ELECTRIC D.C. MOTOR. THE POSITION SETTING OF THE VALVE WILL BE SET BY A POSITION SENSING DEVICE WHICH IS LOCATED ON THE VALVE IT SELF. IT IS IMPORTANT TO NOTE THAT THIS POSITION SENSING DEVICE IS LOCATED ON THE VALVE SINCE IT ELIMINATE EFFECTS OF BACKLASH IN GEAR SYSTEM. WHEN THIS POSITION SENSING DEVICE IS ACTUATED THE POWER TO THE MOTOR IS CUT OFF. ALSO OLDHAM COUPLING IS USED SO THAT PURE TORQUE IS TRANSMITTED TO THE VALVE.

AS A PART OF AN INITIAL ANALYSIS, IT IS PROPOSED THAT THE VALVE WILL BE OPERATED THROUGH A SPUR GEAR TRAIN. THE OBJECTIVE OF THIS PAPER TO DETERMINE A FEASIBILITY OF USING A SPUR GEARS FOR THE PURPOSE

THE SYSTEM MUST SATISFY THE FOLLOWING CONDITIONS:

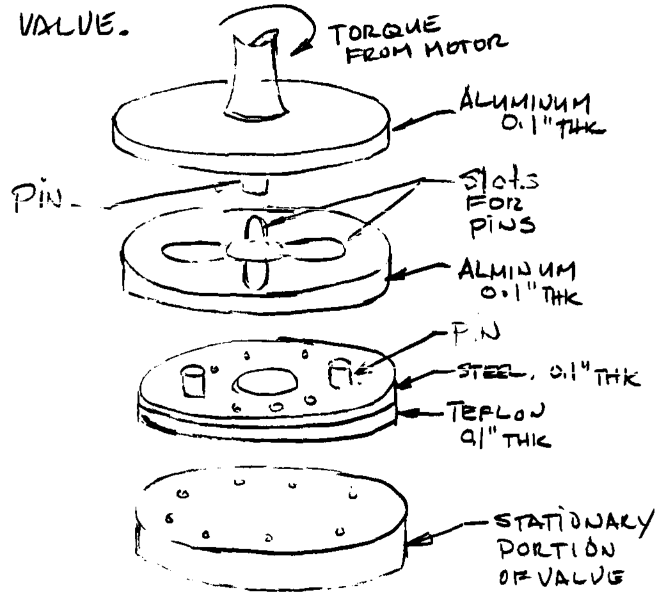

OLDHAM COUPLING
FIG. 1.

1. COAST ANGLE TO BE LESS THAN 0.05°. WHERE COAST ANGLE IS AN ANGLE THE VALVE WILL ROTATE DUE TO INERTIA OF THE SYSTEM AFTER THE POWER TO MOTOR IS CUT OFF.
2. MAXIMUM TIME PERMITTED FOR THE VALVE TO CHANGE POSITION FROM ONE TO THE NEXT CHANNEL IS 0.1 SEC. THIS REQUIREMENT FIXES THE ANGULAR SPEED OF THE VALVE. ($10\pi/4$ rad/sec)

SINCE THE COAST ANGLE IS SO SMALL IT IS INTUITIVELY EXPECTED THAT SMALL EFFECTS, SUCH AS FRICTION IN GEAR TRAIN, EFFICIENCY OF OF THE SYSTEM, MOMENT OF INERTIA OF GEAR TRAIN, WOULD PLAY AN IMPORTANT ROW IN DETERMINING A MOTOR SIZE, GEAR TRAIN CONFIGURATION, ETC. THEREFORE EXPRESSIONS FOR DETERMING SUCH EFFECTS ARE DERIVED FIRST. HOWEVER, IT MUST BE REMINDED THAT THESE EXPRESSIONS WILL NOT BE AN EXACT RELATIONSHIPS SINCE SOME ASSUMPTIONS WILL BE MADE IN DERIVING THEM.

BEFORE DERIVING SUCH EXPESSIONS, LET US SUMMARIZE WHAT ARE THE KNOWN QUANTITIES IS THE SYSTEM.

QUANTITIES KNOWN:

1. DIA. OF VALVE = 1.5 IN.
2. MATERIAL OF VALUE (SEE FIG. 1)
3. COEFFICIENT OF FRICTION IN THE VALVE; $\mu_v = .1$
4. ANGULAR SPEED OF VALVE; $\omega_v = 75$ RPM.
5. FORCE AT WHICH THE ROTATING PORTION OF THE VALVE IS HELD TO THE STATIONARY PORTION; $F_v = 100$#.

QUANTITIES UNKNOWN:

1. MOTOR SPEED, POWER REQUIREMENT, ETC.
2. GEAR CONFIGURATION.

GENERAL ASSUMPTION:

IN ORDER TO SIMPLIFY THE PROBLEM, FOLLOWING ASSUMPTIONS WILL BE MADE. THESE ASSUMPTIONS ARE MADE BY TAKING SIZE AND WEIGHT OF THE SYSTEM INTO CONSIDERATION;

1. THE PINION GEARS IN GEAR TRAIN WILL BE IDENTICAL, AND DIAMETER WILL BE SET AT 0.2 IN.
2. THICKNESS OF PINION AND DRIVEN GEARS IS THE SAME.
3. THE MAXIMUM GEAR STAGE REDUCTION WILL BE 4.
4. SINCE THERE IS NO LUBRICANT PRESENT IN THE VALVE, FRICTION WILL BE OF COULOMB FRICTION, AND INDEPENDENT OF VALVE SPEED.
5. THICKNESS OF GEARS WILL BE 0.5 IN.
   THIS ASSUMPTION WAS MADE BASED UPON CALCULATION USING LEWIS' FORMULA WITH TRANSMITTED TORQUE OF 15-lb·in BY PINION.
6. GEARS WILL BE MADE OF STEEL ($\rho = .282\ \mathrm{lbm/in^3}$)

DERIVATION OF BASIS RELATIONSHIPS.

I. DETERMINATION OF COAST ANGLE:

CONSIDER VALVE AS A FLYWHEEL.

MOMENT OF INERTIA = I

INITIAL ANG. SPEED = W_0

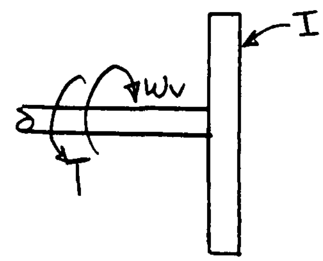

FIG. 2

TOTAL ENERGY REQUIRED TO STOP THE FLYWHEEL IS

$$E = \frac{1}{2} I W_0^2 \longrightarrow \text{KINETIC ENERGY OF THE WHEEL AT START.}$$

IN ORDER TO STOP THE WHEEL, TORQUE T MUST BE APPLIED.

$$\therefore \quad E = \int_{\theta_1}^{\theta_2} T \, d\theta = \frac{1}{2} I W_0^2$$

SINCE T IS CONSTANT;

$$T(\theta_2 - \theta_1) = \frac{1}{2} I W_0^2 \quad \text{OR} \quad \boxed{\Delta\theta = \frac{I W_0^2}{2T}} \text{------(I)}$$

$\Delta\theta$ = COAST ANGLE

I = MOMENT OF INERTIA OF SYSTEM REFLECTED TO THE VALVE.

T = TORQUE IN VALVE, GEAR TRAIN, AND MOTOR.

W_0 = ANGULAR SPEED OF THE VALVE.

NOTE: SINCE TORQUE & W_0 ARE FIXED ONLY I CAN BE VARIED.

II. RELATIONSHIP BETWEEN GEAR RATIO AND MOMENT OF INERTIA

CONSIDER A PAIR OF PINION AND DRIVEN GEARS WHOSE RADII ARE r AND R, RESPECTIVELY.

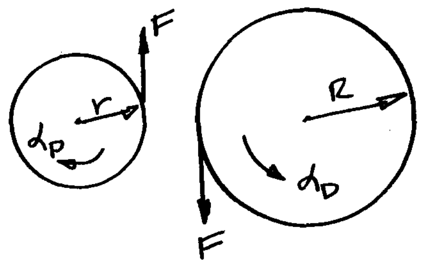

ASSUME THAT THE PINION HAS AN ACCELERATION OF α_P. THEN THE ANGULAR ACCELERATION OF THE DRIVEN GEAR IS RELATED TO α_P BY THE EXPRESSION:

$$\alpha_D = \frac{r}{R}\alpha_P = \frac{1}{n}\alpha_P \;; \quad \text{WHERE } n \text{ IS GEAR RATIO. } n>1;$$

THEN TORQUE ON THE PINION IS

$$T_P = I_P \alpha_P \;; \quad \text{WHERE } I = \text{MOMENT OF INERTIA}$$

ALSO TORQUE ON THE DRIVEN GEAR IS:

$$T_D = I_D \alpha_D = I_D\left(\frac{\alpha_P}{n}\right)$$

BUT TORQUE ON THE PINION IS ALSO EQUAL TO

$$T_P = Fr$$

AND ON THE DRIVEN GEAR:

$$T_D = FR.$$

THEREFORE $\quad \frac{T_P}{T_D} = \frac{\cancel{F}r}{\cancel{F}R} = \frac{I_P \cancel{\alpha_P}}{I_D \cancel{\alpha_P}/n} = 1/n$

SO WE HAVE $\quad \boxed{I_D = n^2 I_P}$ ---- (II)

FROM THIS EXPRESSION, IT CAN BE SHOWN THAT MOMENT OF INERTIA OF A GEAR TRAIN AND LOAD REFLECTED AT MOTOR SHAFT IS

$$I = I_1 + (I_2+I_3)\left(\frac{1}{n_1}\right)^2 + (I_4+I_5)\left(\frac{1}{n_1}\right)^2\left(\frac{1}{n_2}\right)^2 + \cdots \quad \text{(III)}$$

(SEE FIG. 3)

FOR GEAR TRAIN OF TWO STAGES EQ.(III) IS

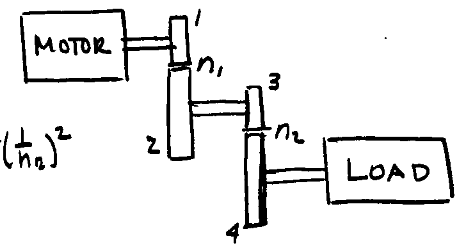

FIG. 3

$$I_m = I_1 + (I_2+I_3)\left(\frac{1}{n_1}\right)^2 + (I_4+I_{LOAD})\left(\frac{1}{n_1}\right)^2\left(\frac{1}{n_2}\right)^2$$

WHERE

I_m = MOM. OF INERTIA OF SYSTEM REFLECTED AT MOTOR SHAFT.

I_i = MOM. OF INERTIA OF GEAR # i

I_{LOAD} = MOM. OF INERTIA OF LOAD

n_i = GEAR RATIO AT STAGE i

NOTE FROM EQ. (I), THE COAST ANGLE IS MINIMIZED WHEN MOMENT OF INERTIA IS MINIMIZED. THEREFORE IT IS DESIRED TO MINIMIZE THE MOMENT OF INERTIA OF GEAR TRAIN.

IF WE LET N_i = REDUCTION RATIO FROM MOTOR TO iTH PINION.

ABOVE EQUATION CAN BE REWRITTEN IN THE FORM

$$I_m = I_1 + (I_2+I_3)\left(\frac{1}{N_1}\right)^2 + (I_4+I_{LOAD})\left(\frac{1}{N_2}\right)^2$$

TO MINIMIZE THIS INERTIA WE SET

$$\frac{\partial I_m}{\partial N_i} = 0$$

NOTE THAT MOMENT OF INERTIAS OF GEARS #2 AND #3 ARE RELATED BY

$$I_2 = \left(\frac{r_2}{r_3}\right)^4 I_1$$

SINCE WE ASSUMED THAT RADIUS OF PINION GEARS ARE THE SAME, i.e. $r_1 = r_3$, WE HAVE

$$I_2 = n_1^4 I_1 \quad ; \quad n_1 = N_1 \; ; \; n_2 = \frac{N_2}{N_1}$$

SO $$I_m = I_1 + I_1\left(N_1^2 + \frac{1}{N_1^2}\right) + \frac{N_2^2}{N_1^4} I_1 + \frac{I_{LOAD}}{N_2^2}$$

$$\therefore \frac{\partial I_m}{\partial N_1} = I_1\left[2N_1 - 2\frac{1}{N_1^3} - 4\frac{N_2^2}{N_1^5}\right] = 0$$

$$= I_1\left[N_1^6 - N_1^2 - 2N_2^2\right] = 0$$

III EFFICIENCY OF GEAR TRAIN

IN DERIVING AN EXPRESSION FOR EFFICIENCY, IT WILL BE ASSUMED THAT MAJORITY OF TORQUE LOSS OCCURS IN SHAFT BEARING, AND FRICTION IN BEARING IS COULOMB FRICTION.

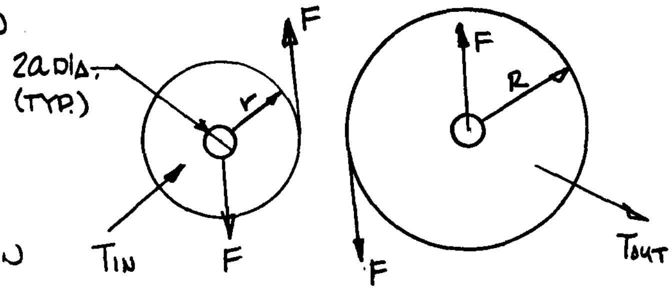

FIG 4.

IF F IS A FORCE FORCE ACTING ON GEAR TEETH, THERE WILL A REACTION AT THE BEARING.

THEN FRICTIONAL TORQUE IS

$$T_f = \mu F a \qquad ; \quad \mu = \text{FRICTION FACTOR}$$

a = RADIUS OF SHAFT.

T_f = FRICTIONAL TORQUE

ALSO WE HAVE

$$F = \frac{T_{IN} - T_f}{r}$$

$$\therefore \; T_{IN} = (Fr + \mu F a) = Fr\left(1 + \frac{\mu a}{r}\right)$$

NOW LOOKING AT DRIVEN GEAR:

$$T_{OUT} = FR - \mu F a = FR\left(1 - \frac{\mu a}{R}\right)$$

$$\therefore \; \frac{T_{IN}}{T_{OUT}} = \frac{\cancel{F} r\left(1 + \frac{\mu a}{r}\right)}{\cancel{F} R\left(1 - \frac{\mu a}{R}\right)} = \frac{1}{n}\,\frac{(r + \mu a)\left(\frac{1}{r}\right)}{(R - \mu a)\left(\frac{1}{R}\right)} \quad ; \text{ WHERE } n = \frac{R}{r}$$

$$\frac{T_{in}}{T_{OUT}} = \frac{(r + \mu a)}{(R - \mu a)} = \frac{(r + \mu a)}{(nr - \mu a)}$$

$$\therefore \; T_{OUT} = T_{in}\left(\frac{nr - \mu a}{r + \mu a}\right)$$

IF THERE WAS NO FRICTION:

$$(T_{OUT})_{IDEAL} = n\,T_{IN}.$$

$$\therefore \; \eta = \frac{T_{OUT}}{(T_{OUT})_{IDEAL}} = \frac{\cancel{T_{in}}\left(\frac{nr - \mu a}{r + \mu a}\right)}{\cancel{T_{in}}\; n} = \frac{1}{n}\left[\frac{nr - \mu a}{r + \mu a}\right] \quad \text{----(IV)}$$

IT WILL BE ASSUMED AT EFFICIENCY OF EACH STAGE WILL BE THE SAME. SO EFFICIENCY OF A GEAR TRAIN OF m STAGES IS:

$$\boxed{\eta_{TOTAL} = \eta_{STAGE}^{m}}$$

IV FRICTION IN BEARING

FROM LAST SECTION
WE HAVE

$$T_{OUT} = FR - T_f$$

AND

$$F = \frac{T_{in} - T_f}{r}$$

$$T_{IN} = \frac{T_{OUT}}{\eta n}$$

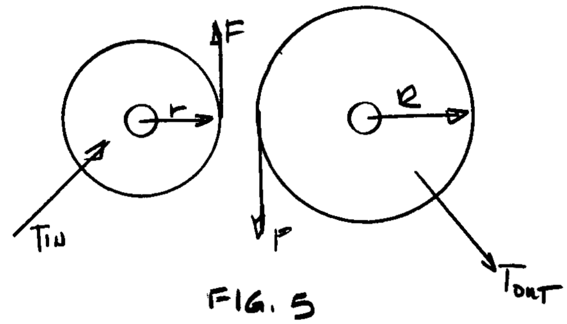

FIG. 5

$$\therefore \quad T_f = FR - T_{OUT} = \left(\frac{T_{in} - T_f}{r}\right)R - T_{OUT}$$

$$T_f = n(T_{in} - T_f) - T_{OUT}$$

SO
$$T_f(1+n) = nT_{IN} - T_{OUT}$$

$$= \cancel{n}\left(\frac{T_{OUT}}{\eta \cancel{n}}\right) - T_{OUT}$$

$$= T_{OUT}\left(\frac{1}{\eta} - 1\right) = T_{OUT}\left(\frac{1-\eta}{\eta}\right)$$

$$\therefore \quad \boxed{T_f = \frac{T_{OUT}(1-\eta)}{\eta(1+n)}} \quad \text{------------} \quad (V)$$

ALSO IN THIS CASE IT IS ASSUMED THAT DOMINANT FRICTION LOSS WILL OCCUR IN BEARING. I.E. IT IS ASSUMED THAT THERE IS NO LUBRICATION AND THERE WILL BE NO LUBRICANT FILM DEVELOPED,

AT THIS POINT LET US ESTIMATE WHAT IS THE MAGNITUDE OF EFFICIENCY.

USING TYPICAL VALUES:

$\mu = .15$ COEFF. OF FRICTION
$a = .05''$ DIA. OF SHAFT.
$n = 4$ GEAR RATIO
$r_p = .10''$

$$\mu = \frac{1}{n}\left[\frac{nr - \mu a}{r + \mu a}\right] = \frac{1}{4}\left[\frac{4(.1) - (.15)(.025)}{.1 + (.15)(.025)}\right] = .95 = 95\%$$

THIS EFFICIENCY IS A REASONABLE FOR THIS TYPE OF GEAR.

ANALYSIS

IF ONE WISHES TO ANALYZE THIS PROBLEM AND ARRIVE AT SOME OPTIMUM SYSTEM, HE MUST RESORT TO A "TRIAL-ERROR" METHOD OF ANALYSIS. SINCE SIZE, SPEED, TORQUE OUTPUT, ETC. OF MOTOR AND GEAR CONFIGULATION ARE NOT KNOWN, ONE CAN CHOOSE ALMOST "INFINITE" NUMBER OF DIFFERENT COMBINATION OF VARIABLES. HOWEVER, SINCE THE PURPOSE OF THIS PAPER IS TO DETERMINE A FEASIBILITY OF USE OF SPUR GEAR TRAIN FOR THIS SYSTEM, WE WILL NOT TAKE OPTIMIZATION OF THE SYSTEM IN DETAIL. INSTEAD A TYPICAL EXAMPLE CALCULATION WILL BE MADE TO OBTAIN SOME IDEAS OF FEASIBILITY OF THE SYSTEM.

BEFORE GOING INTO A FORMAL ANALYSIS OF THE SYSTEM LET US IDEALIZE THE SYSTEM NEGLECTING ALL SMALL EFFECTS TO MAKE A ROUGH ESTIMATE OF WHAT IS TO EXPECTED.

FIRST OF ALL LET US CALCULATE QUANTITIES THAT ARE FIXED.

1. TORQUE IN VALVE:

$\mu = .10$ COEFF. OF FRICTION (STATIC & DYNAMIC)
$N = 100$ lbf. NORMAL FORCE

$\therefore \; dF_f = fN\,dA$
$\quad = fN(2\pi r\,dr)$

TORQUE, $dT_f = r\,dF_f$

$\therefore \; dT_f = 2\pi f N r^2 dr$

INTEGRATING:

$$T_f = 2\pi f N \int_0^{.75} r^2 dr$$
$$= 2\pi(.1)(100)\left[\frac{r^3}{3}\right]_0^{.75}$$
$$= \frac{2}{3}\pi(10)(422)$$
$$\underline{\underline{T_f = 8.84 \text{ lbf-in}}}$$

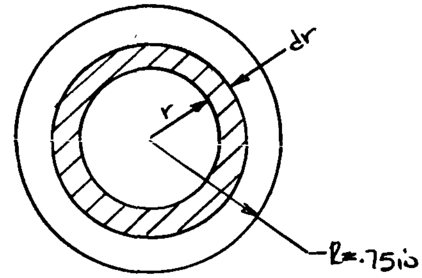

FIG. 6

2. MOMENT OF INERTIA OF THE VALVE:

ASSUMING THAT THE VALVE CONSISTS OF DISKS.

$\rho_{AL} = 0.092$ lbm/in³

$\rho_{STL} = 0.282$ lbm/in³

$\rho_{TEF} = 0.072$ lbm/in³

MOMENT OF INERTIA OF A DISK:

$$I = \tfrac{1}{2} m r^2$$

$$m = \pi r^2 t \rho$$

m = MASS OF DISK
r = RAD. OF DISK
t = THICKNESS OF DISK
ρ = DENSITY

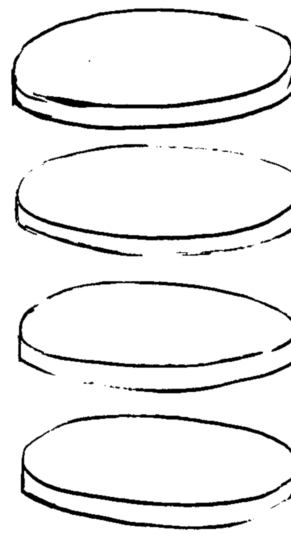

FIG. 7

MOMENT OF INERTIA OF THE VALVE IS THE SUM OF INDIVIDUAL MOMENT OF INERTIA.

SINCE r AND t ARE COMMON TO ALL PIECES, WE HAVE

$$I_{VALVE} = \tfrac{1}{2}\pi r^4 t\,(\rho_{STL} + 2\rho_{AL} + \rho_{TEF})$$

$$= \frac{\tfrac{1}{2}\pi(.75)^4(.1)[0.282 + 2(.092) + .072]}{(32.2)(12)} \quad \text{SLUG-IN}^2$$

$$\underline{I_V = 6.92 \times 10^{-5} \text{ SLUG-IN}^2}$$

3. MOMENT OF INERTIA OF PINION:

$\rho_{STL} = 0.282$ lbm/in³
$r_P = 0.10$ in
$t_P = 0.05$ in

$$I_P = \tfrac{1}{2} m r_P^2 = \tfrac{1}{2}(\pi r_P^2 t_P \rho_P)(r_P^2) = \tfrac{1}{2}\pi(.1)^4(.05)(.282)/(32.2)(12)$$

$$\underline{I_P = 5.73 \times 10^{-9}} \text{ SLUG-IN}^2$$

A. Rough Estimate of Coast Angle:

In order to begin assume motor speed:

Let motor speed $W_m = 6000$ RPM.

Vavle speed $W_v = 75$ RPM.

Total speed reduction $N = 6000/75 = 80$

Speed reduction per stage $n = 4$.

No. of stages req'd $m = \dfrac{\ln 80}{\ln 4} = 3.15$

$\therefore$ Let $\underline{m = 3}$

Then motor speed becomes $W_M = 3^4(75) = 4800$ RPM.

Total speed reduction $N = 64$.

Torque in value $= 8.84$ lbf-in;

Torque req'd motor $= 8.84/64$

$= .138$ lbf-in

$= 2.21$ oz-in

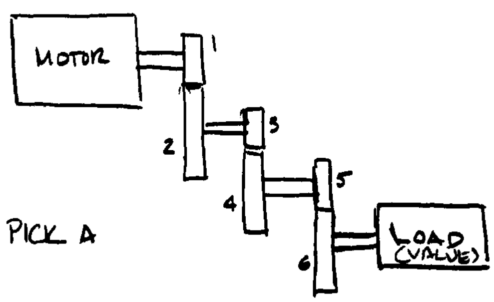

FIG. 8

Knowing speed and torque req'd, pick a motor from a catologue.

Let us use Barber-Colman D.C. Motor HYLM-43400

This motor has armature moment of inertia $I_m = 4.65 \times 10^{-6}$ slug-in^2

Total moment of inertia reflected at the valve:

$$(I_{Total})_v = (n^3)^2(I_m + I_1) + (n^2)^2(I_2 + I_3) + n^2(I_4 + I_5) + I_6 + I_v$$

But $I_1 = I_3 = I_5 = I_p = 5.73 \times 10^{-9}$ slug-in^2.

Also it can be shown that

$$I_2 = I_4 = I_6 = n^4 I_p$$

$$\therefore (I_{Total})_v = n^6(I_m + \overset{\text{NEGLECT}}{\cancel{I_p}}) + (n^4)(n^4 I_p + I_p) + n^2(n^4 I_p + I_p) + \overset{\text{NEGLECT}}{\cancel{I_p}} + I_v$$

Substituting $n = 4$, $I_p = 5.73 \times 10^{-9}$ slug-in^2, $I_m = 4.65 \times 10^{-6}$ slug-in^2

$$(I_{Total})_v = \underbrace{.0191}_{\text{MOTOR}} + \underbrace{.0004}_{\text{GEAR TRAIN}} + \underbrace{.0000696}_{\text{FROM VALVE}} = \underline{\underline{.0195}} \ \underline{\text{slug-in}^2}$$

Note that moment of inertia of the motor is the dominating term.

NOW WE CAN CALCULATE THE COAST ANGLE:

$$\Delta\theta = \frac{(I_{TOTAL})_V W_V^2}{2\,T_V} \quad ; \qquad W_V = \text{VALVE SPEED} = 75 \text{ RPM} = \frac{10\pi}{4} \text{ RAD/SEC}$$

$$T_V = \text{TORQUE IN VALVE} = 8.84 \text{ lbf-in}$$

$$= \frac{(.0195)\left(\frac{10\pi}{4}\right)^2}{2(8.84)}$$

$$\underline{\Delta\theta = .068 \text{ rad}}$$

SPECIFIED $\Delta\theta = 0.05° = .000873$ rad.

∴ THE CALCULATED COAST ANGLE IS ABOUT 78 TIMES AS GREAT AS SPECIFIED VALUE.

FROM THIS RESULT IT IS OBVIOUS THAT INCLUSION OF SMALL EFFECTS WILL NOT IMPROVE THE RESULT SIGNIFICANTLY. THE SYSTEM, AS IT IS NOW, IS OBVIOUSLY NOT FEASIBLE. IF THE SYSTEM TO BE FEASIBLE, AT ALL, SOME WAY TO BRAKE THE MOTOR MUST BE PROVIDED.

HOWEVER, BEFORE CONSIDERING BRAKING OF THE MOTOR LET US CALCULATE THE COAST ANGLE WITH SMALL EFFECTS TO SEE HOW SIGNIFICANT THEY ARE.

B. COAST ANGLE WITH SMALL EFFECTS INCLUDED:

USING THE SAME MOTOR

$W_M = 4800$ RPM
$W_V = 75$ RPM
$I_M = 4.65 \times 10^{-6}$ SLUG-IN^2
$I_V = 6.96 \times 10^{-5}$ SLUG-IN^2
$I_P = 5.73 \times 10^{-7}$ SLUG-IN^2

FOR THIS CASE DIAMETERS OF DRIVEN GEARS MAY NOT BE EQUAL.

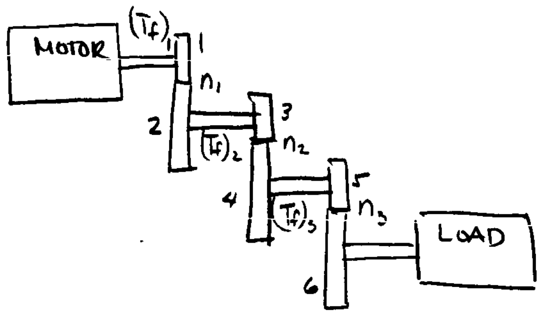

FIG. 8 REPEATED

1. LET US MINIMIZE THE MOMENT OF INERTIA OF THE GEARTRAIN.

EXPRESSION FOR TOTAL MOMENT OF INERTIA REFLECTED AT THE MOTOR BECOMES:

OMITTING INTERMEDIATE STEPS (SEE PG. 6), WE HAVE:

$$(I_{TOTAL})_m = I_1 + I_1 N_1^2 + I_3/N_1^2 + I_3\left(\frac{N_2^2}{N_1^4}\right) + \frac{I_5}{N_2^2} + I_5\left(\frac{N_3^2}{N_2^4}\right) + I_v\left(\frac{1}{N_3^2}\right) \; ; \quad \text{NOTE } N_3 = N = \text{CONST.}$$

SETTING:

$$\frac{\partial (I_{TOT})_m}{\partial N_1} = 0 = I_P\left(N_1^6 - \cancel{N_1^2}^{\text{NEGLECT}} - 2N_2^2\right) \quad ; \quad I_1 = I_3 = I_5 = I_P$$

$$\frac{\partial (I_{TOT})_m}{\partial N_2} = 0 = I_P\left(\frac{N_2^6}{N_1^4} - \cancel{N_2^2}^{\text{NEGLECT}} - 2N_2\right)$$

SINCE WE HAVE TWO EQUATIONS WITH TWO UNKNOWNS, N_1 AND N_2 MAY BE SOLVED. SOLVING FOR N_1 AND N_2:

$$N_1 = (4N)^{1/7} = n_1 \qquad \text{WHERE } N = \text{TOTAL REDUCTION RATIO} = 64$$

$$N_2 = \frac{4(N)^{3/4}}{\sqrt{2}} = N_1 n_2$$

SUBSTITUTING $N = 64$:

$N_1 = n_1 = \left(\frac{r_2}{r_p}\right) = 2.21 \qquad \therefore \; \underline{r_2 = .221 \text{ in}}$

$N_2 = N_1 n_2 = 7.6 \qquad \therefore \; n_2 = 3.44 = \left(\frac{r_4}{r_p}\right), \; \underline{r_4 = .344 \text{ in}}$

$N_3 = N = N_2 n_3 \qquad \therefore \; n_3 = 8.43 = \left(\frac{r_6}{r_p}\right), \; \underline{r_6 = .843 \text{ in}}$

TOTAL MOMENT OF INERTIA REFLECTED AT THE VALVE:

$$(I_{TOTAL})_v = (I_m + I_p)n_1^2 + (I_2 + I_3)(n_1)^2(n_2)^2 + (I_4 + I_5)(n_1)^2(n_2)^2(n_3)^2 + I_6 + I_v$$

GOING THROUGH SIMILAR PROCESS AS BEFORE:

$$(I_{TOTAL})_v = \underbrace{.0191}_{\text{MOTOR}} + \underbrace{.000165}_{\text{GEAR}} + \underbrace{.0000988}_{\text{VALVE}} \quad \text{SLUG-in}^2$$

$$\underline{(I_{TOTAL})_v = 1.926 \times 10^{-2} \quad \text{SLUG in}^2}$$

NOTE THAT THERE ISN'T SIGNIFICANT CHANGE IN TOTAL MOMENT OF INERTIA.

2. NOW USING EQ. (V) CALCULATE FRICTION IN GEARTRAIN:

$$(T_f)_3 = \frac{(T_{OUT})_3(1-\eta)}{\eta(1+n_3)} \quad ; \quad (T_{OUT})_3 = 8.84 \text{ lbf-in}, \quad \eta = 95\%, \quad n_3 = 8.43$$

$$\underline{(T_f)_3 = .0493 \text{ lbf-in}}$$

FRICTION THIRD STAGE

SIMILARLY:

$\underline{(T_f)_2 = .0104 \text{ - lb-in}}$

$\underline{(T_f)_1 = .005 \text{ - lb-in}}$

NOTE: $(T_{OUT})_k = \dfrac{(T_{OUT})_{k+1}}{\eta\,(n)_{k+1}}$

REFLECTING FRICTIONAL TORQUES TO THE VALVE:

$$(T_f)_{3v} = (T_f)_3 \eta n_3 = (.0493)(.95)(8.43) = .396 \text{ lbf-in}$$

$$(T_f)_{2v} = (T_f)_2 \eta^2 n_2 n_3 = (.0104)(.95)^2(8.43)(3.44) = .272 \text{ lbf-in}$$

$$(T_f)_{1v} = (T_f)_1 \eta^3 n_1 n_2 n_3 = (.005)(.95)^3(64) = .274 \text{ lb-in}$$

TOTAL FRICTIONAL TORQUE IN GEAR TRAIN AT VALVE = .942 lb-in

WITH THESE SMALL EFFECTS COAST ANGLE WILL BE CALCULATED:

$$\Delta\theta = \frac{(I_{Total})_v \, \omega_v^2}{2(T_v + T_f)}$$

$$\Delta\theta = \frac{(1.926\times10^{-2})\left(\frac{10\pi}{4}\right)^2}{2(8.84+.942)} = .0606 \text{ RAD}$$

COMPARING THE TWO RESULTS, WE CAN OBSERVE THAT THERE IS ABOUT 12% DIFFERENCE BETWEEN THEM. ALTHOUGH THE DIFFERENCE IN THIS PARTICULAR CASE DOES NOT ALTER THE PROBLEM MUCH, BUT IF THE CALCULATED COAST ANGLE WAS IN THE SAME ORDER OF MAGNITUDE AS THE SPECIFIED VALUE WE CAN SEE THAT THESE SMALL EFFECTS CAN MAKE A WORLD OF DIFFERENCE IN SOLUTION OF ANALYSIS.

NOTE THAT MOST SIGNIFICANT CHANGE FROM INCREASE IN TORQUE DUE TO FRICTION IN GEAR TRAIN, AND EFFECT OF MINIMIZING THE MOMENT OF INERTIA DOES NOT CONTRIBUTE MUCH.

NOW THE QUESTION "CAN THIS SYSTEM BE MADE FEASIBLE?" AS IT WAS MENTIONED BEFORE, IN ORDER TO MAKE THIS SYSTEM WORK WE MUST NEGATE THE EFFECT OF MOTOR ROTOR INERTIA BY SOME MEANS SINCE IT IS THE DOMINANT CAUSE OF TROUBLE. HOW CAN THIS BE ACCOMPLISHED? TWO MOST OBVIOUS METHODS COMES TO MY MIND.

1. APPLY A TORQUE TO THE ROTOR OF THE MOTOR TO STOP IT IN TIME. THERE IS A ELECTRO-MAGNETIC DEVICE WHICH CAN BE INSTALLED IN SERIES WITH THE MOTOR SO THAT WHEN POWER TO THE MOTOR IS CUT OFF THIS DEVICE IS ENERGIZED THUS APPLYING BRAKING TORQUE TO THE SHAFT OF THE MOTOR.

2. SECOND METHOD IS TO ELIMINATE THE CAUSE OF TROUBLE. THAT IS, SOMEHOW DISCONNECT THE MOTOR FROM THE SYSTEM WHEN POWER TO THE MOTOR IS CUT OFF. THIS CAN ALSO BE DONE WITH A SIMILAR ELECTRO-MAGNETIC CLUTCH.

LET US CONSIDER THE FIRST METHOD, AND SEE IF WE CAN FIND SUCH A DEVICE WHICH WILL SUPPLY ENOUGH BRAKING TORQUE TO OVERCOME MOTOR AND ITS OWN MOMENT OF INERTIA. FROM EQ. (I) WE CAN SOLVE FOR I/T AND USE THAT EXPRESSION TO TEST THE REQUIREMENT OF BRAKING DEVICE:

EQ. (I) --- $\Delta\theta = \dfrac{I\omega_v^2}{2T}$

SOLVING FOR I/T: $\underline{I/T = \dfrac{2\Delta\theta}{\omega_v^2}}$

ALL THE VALUES IN THIS EXPRESSION MUST REFLECTED TO THE MOTOR SHAFT.

$$(\Delta\theta)_M = (\Delta\theta)_V(64) = (.00087)(64) = .0558 \text{ RAD}$$

$$(\omega_V)_m = 4800 \text{ RPM.} = 160\pi \text{ rad/sec.}$$

$$(I_{TOT})_M = (.0195)(64)^2 = 4.76 \times 10^{-6} \text{ slug-in}^2$$

$$(T_V)_M = \frac{8.84}{64} = .138 \text{ lbf-in}$$

I IN ABOVE IN ABOVE EXPRESSION EQUAL TO THE SUM MOMENT OF INERTIAS OF THE SYSTEM AND OF BRAKING DEVICE. ALSO T IS THE SUM OF TORQUE IN THE SYSTEM AND BRAKING TORQUE SUPPLIED BY THE DEVICE.

$$\therefore \frac{[(I_{TOT})_M + I_{BRAKE}]}{[(T_V)_M + T_{BRAKE}]} = \frac{2(\Delta\theta_V)_M}{(\omega_V)_M} = \frac{2(.0558)}{(160\pi)^2}$$

$$\frac{4.76\times10^{-6} + I_{BR}}{.138 + T_{BR}} = 4.4\times10^{-7}$$

THIS EXPRESSION TELLS US THAT IF WE CAN FIND A BRAKING DEVICE WITH PROPERTY SUCH ~~THAT~~ WHEN ITS MOMENT OF INERTIA AND BRAKING TORQUE ARE SUBSTITUTED INTO IT AND IF THE LEFT HAND SIDE OF THE EXPRESSION COMES TO BE SMALLER THAN RIGHT HAND SIDE THEN THE DEVICE WILL SUCCEED IN STOPPING THE VALVE WITH IN SPECIFIED COAST ANGLE.

AFTER CHECKING THROUGH VARIOUS TYPES OF ELECTRO-MAGNETIC BRAKES, I WAS NOT ABLE TO FIND SUCH A DEVICE WHICH SATISTIFIES THE EXPRESSION DRIVED. IN THE PROCESS OF CHECKING THROUGH THESE DEVICES IT WAS NOTED THAT AS BRAKING TORQUE OF SUCH DEVICE INCREASES ITS SIZE, AND THEREFORE ITS MOMENT OF INERTIA INCREASES, AT MUCH FASTER RATE. THEREFORE IT MUST BE CONCLUDED THAT THIS TYPE OF DEVICE IS NOT FEASIBLE FOR THIS PARTICULAR APPLICATION.

NOW LET US CONSIDER THE SECOND METHOD WHERE CLUTCH IS USED TO DISCONNECT THE MOTOR SHAFT FROM THE SYSTEM.

LET US DERIVE A SIMILAR EXPRESSION AS IN LAST SECTION.

$$I/T = \frac{2\Delta\theta}{\omega^2}$$

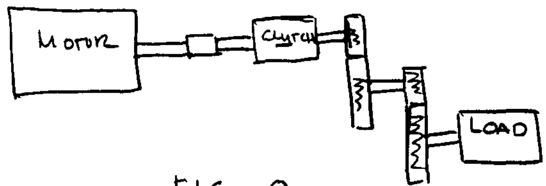

FIG. 9

FOR THIS CASE

$$I = I_{CLUTCH} + (I_{G.T.})_M \qquad , (I_{G.T.})_M = (.00047)\left(\frac{1}{64}\right)^2 = 1.15 \times 10^{-7} \text{ SLUG-IN}$$

(I OF MOTOR EXCLUDED)

$$T = T_{CLUTCH} + (T_V)_M \qquad (T_V)_M = .138 \text{ lbf-in.}$$

$$\therefore \quad \frac{1.15 \times 10^{-7} + I_{CLUTCH}}{.138 + T_{CLUTCH}} = 4.47 \times 10^{-7}$$

FOR THE SAME REASON AS BEFORE WE MUST CONCLUDE THAT THIS TYPE OF DEVICE WILL NOT WORK, ALSO. THIS WAS EXPECTED SINCE MOMENT OF INERTIA OF SUCH A DEVICE IS USUALLY GREATER THAN THAT OF THE MOTOR. ALTHOUGH THESE DEVICES ARE EQUIPPED TO APPLY A BRAKING TORQUE BUT INCREASE IN BRAKING TORQUE IS NOT ENOUGH TO OVERCOME THE INCREASE IN MOMENTUM OF INERTIA.

HOWEVER, IF WE CHANGE THE ARRANGEMENT AND LOCATE A CLUTCH BETWEEN THE VALUE AND THE GEAR TRAIN I WAS ABLE TO FIND ONE DEVICE WHICH WOULD STOP THE VALVE WITHIN SPECIFIED COAST ANGLE.

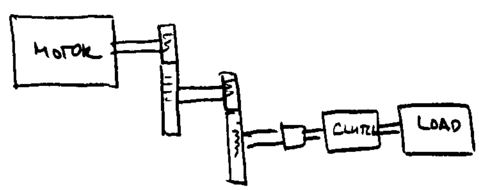

FIG. 10

SPECS. ON THE DEVICE ARE:

"AUTOTRONIC INC". TYPE "MBB" CLUTCH-BRAKE

WEIGHT = 16. OZ

BRAKE TORQUE = 200 OZ-IN = 12.5 lb-in.

CLUTCH TORQUE = 180 OZ-IN = 11.25-lb-in

MOMENT OF INERTIA = $90. \times 10^{-6}$ SLUG-IN^2

LET US CALCULATE THE COAST ANGLE USING ABOVE DATA:
SINCE THE CLUTCH IS LOCATED BETWEEN THE VALVE AND GEAR TRAIN, WHEN IT IS ENERGIZED THE GEAR TRAIN AND MOTOR IS SET FREE. THEREFORE ONLY INERTIA FORCES THAT THE CLUTCH HAS TO OVERCOME ARE THAT OF THE VALVE AND THE CLUTCH ITSELF.

SUBSTITUTING DATA IN COAST ANGLE EQUATION:

$$\Delta\theta = \frac{I\omega_v^2}{2T} = \frac{(I_{clutch} + I_v)(\omega_v^2)}{2(T_{clutch} + T_v)}$$

$$= \frac{(90\times10^{-6} + 69.6\times10^{-6})\left(\frac{10\pi}{4}\right)^2}{2(8.84 + 12.5)}$$

$$\underline{\delta\theta = .000393 \text{ rad}} < .00087 \text{ rad.}$$

NOTE THAT IN CALCULATING THIS VALUE, THE SMALL EFFECTS DO NOT COME INTO PLAY SINCE THE DRIVING SYSTEM HAS BEEN DISCONNECTED FROM THE VALVE. HOWEVER SMALL EFFECTS WITHIN THE CLUTCH DEVICE WAS NEGLECTED SO THE CALCULATED COAST ANGLE IS ON THE CONSERVATIVE SIDE, ALTHOUGH BY NOT MUCH.
THE SIZE OF THIS PARTICULAR UNIT IS 2" x 2" DIA. AND WEIGHS ONE POUND. THE POWER REQUIRED TO OPERATE IS 4.2 WATT. TAKING THESE FACTORS INTO ACCOUNT IT APPEARS THAT THIS SYSTEM IS NOT VERY FEASIBLE.

THERE IS ONE OTHER SIMPLE METHOD OF BRAKING A D.C. MOTOR WHICH IS KNOWN AS DYNAMIC BREAKING. THIS IS ACCOMPLISHED BY SHORT CIRCUITING THE INPUT LEADS OF THE MOTOR AT THE INSTANT THE POWER TO THE MOTOR IS CUT OFF. BY SHORT CIRCUITING THE INPUT LEADS, THE MOTOR WILL ACTS AS A GENERATOR AND STRONG BRAKING ACTION MAY BE PRODUCED SINCE THE GENERATED emf OF THE ARMATURE CAUSES CURRENT TO FLOW THROUGH THE INTERNAL RESISTANCE OF THE MOTOR, THUS DISSIPATING THE KINETIC ENERGY OF THE ROTOR A HEAT IN THE RESISTANCE. A DETAILED DISCUSSION OF THIS METHOD WILL NOT BE UNDERTAKEN AT THIS TIME. SINCE TIME AND SPACE ARE LIMITED. IT WILL BE INTERESTING TO SEE WHEATHER THIS METHOD WILL SUCCEEDS IN STOPPING THE VALVE IN TIME. IF IT DOES STOP THE VALVE IN TIME, THIS WILL BE THE CHEAPEST AND MOST SIMPLE METHOD SINCE IT REQUIRES NO POWERSOURCE AND OTHER MECHANICAL DEVICE.

AS IT WAS MENTIONED EARLIER, THERE ARE MANY COMBINATIONS OF VARIABLES WITH ONE CAN ANALYZE THE SYSTEM. IN THIS PAPER ONLY ONE OF THESE WAS CONSIDERED. HOWEVER, IT SEEMED THAT IF SPEED OF THE VALVE IS REDUCED. IT WOULD DECREASE THE COAST ANGLE SINCE W_V^2 APPEARS ON RIGHT HAND SIDE OF EQ.(I). SO SIMILAR CALCULATION WAS MADE WITH WV = 35 RPM. KEEPING THE MOTOR SPEED THE SAME. AS IT TURNED OUT, THE COAST ANGLE CALCULATED FOR THIS CASE WAS LARGER THAN PREVIOUS CASE (.068 rad VS. .08). THIS IS MAINLY DUE TO THE FACT FACT THAT BY REDUCING THE ANGULAR SPEED OF THE VALVE THE OVERALL REDUCTION RATION WAS INCREASED SUCH THAT WHEN MOMENT OF INERTIA OF THE MOTOR ROTOR REFLECTED BACK TO THE VALVE IT WAS MAGNIFIED TO THE EXTENT THAT THE PRODUCT OF $(I)_V$ AND W_V^2 TURNED OUT TO BE LARGER THAN BEFORE. THIS AGAIN EMPHASIZES THE STRONG EFFECT OF MOMENT OF INERTIA OF ROTOR WHEN IT IS REFLECTED BACK TO THE VALVE. IN A WAY, THIS ALSO JUSTIFIES THE DETERMINATION OF FEASIBILITY BASED ON ONLY ONE TYPICAL CALCULATION.

CONCLUSION: BASED ON CALCULATIONS MADE IN THIS PAPER, IT APPEARS THAT SPUR GEAR TRAIN IS NOT SUITED FOR THIS PURPOSE. ALTHOUGH WE ONLY CONSIDERED TWO METHODS OF BRAKING THE MOTOR AND UNDOUBTLY THERE ARE OTHER METHODS WHICH MAY DO THE JOB, I WOULD SUGGEST, BEFORE TRYING TO IMPROVE THIS SYSTEM BY SOME SOPHISTICATED METHOD, TO CONSIDER SOME OTHER GEAR TRAIN SYSTEM. SOME SUGGESTIONS ARE
(1) HARMONIC DRIVE, (2) WARM GEAR, (3) PLANETARY GEAR SYSTEMS.

ONE MAY ALSO CONSIDER DIFFERENT TYPES OF DRIVING MOTORS. ONE POSSIBILITY IS TO USE A DIRECT DRIVE MOTOR WHICH CAN BE ATTACHED DIRECTLY TO THE VALVE. ADVANTAGES OF THIS TYPE OF MOTOR ARE: 1. GEAR TRAIN CAN BE ELIMINATED, 2. SYSTEM ACCURACY INCREASES, 3. FAST RESPONCE TIME. HOWEVER, THIS TYPE OF MOTOR MUST SUPPLY LARGE AMOUNT OF TORQUE SINCE IT IS MOUNTED DIRECTLY TO THE LOAD, AND THIS WILL TEND TO INCREASE ITS WEIGHT. A MOTOR OF THIS OF THIS KIND WHICH WILL SUPPLY ENOUGH TORQUE TO OPERATE THE VALVE WILL WEIGH ABOUT $1\frac{1}{2}$ POUND. THEREFORE MOMENT OF INERTIA OF SUCH MOTOR IS QUITE HIGH.

IN CONCLUSION, LET US REVIEW WHAT I LEARNED FROM THIS ANALYSIS.

1. IT IS ALWAYS GOOD PRACTICE TO MAKE AN ROUGH ESTIMATE OF SOLUTION BY IDEALIZING THE SYSTEM. FOR THIS PARTICULAR

CASE THE ESTIMATED COAST ANGLE WAS SO FAR OFF OF THE SPECIFIED LIMIT WE IMMEDIATELY KNEW THAT SMALL EFFECTS WILL NOT ALTER THE PROBLEM MUCH. IF THE ESTIMATED ANGLE HAD BEEN IN THE SAME MAGNETUDE AS THE SPECIFIED VALUE, WE'VE HAD TO INCLUDE THE SMALL EFFECTS AND GO THROUGH THE ANALYSIS AGAIN.

2. ALWAYS TRY TO DETERMINE WHAT WILL BE THE MOST DOMINANT FACTOR IN THE SYSTEM BEFORE ATTEMPTING TO ANALYZE THE SYSTEM.

3. FOR THIS TYPE OF ANALYSIS WHERE ONE IS NOT REALLY INTERESTED IN EXACT SOLUTION, IT WILL BE BETTER IDEA TO NEGLECT THE SMALL EFFECTS SINCE THIS WILL GIVE SOLUTION ON CONSERVATIVE SIDE.

FINALLY, IN MY OPINION, SPUR GEAR TRAIN SPEED REDUCER FOR THIS PURPOSE IS NOT VERY FEASIBLE.

REFERENCES:

1. GIBSON, CONTROL SYSTEM COMPONENTS, McGraw-Hill
2. MAXWELL, KINEMATICS AND DYNAMICS OF MACHINERY.
3. PETERSON, "POWER GEAR TRAINS" MACHINE DESIGN, JUNE 1954.

ANALYSIS

OF A

MULTIVATOR MODULE

William A. Ribich
November 19, 1964

I. DESCRIPTION OF THE VALVE

The subject of this analysis is shown in Fig. 1. Prior to activation slide A is at the top of its enclosing chamber as is Slide B. Passage D is open and passage T is closed at this time. Upon activation a supply pressure P_s is applied, forcing slide A into the position shown. For the instant of time shown, slide B has just begun to move, forcing the fluid beneath it through passage T into chamber 3.

Both the valve casing and the slides are made from 303 stainless. The slides have a radial clearance of approximately one mil. A high vacuum grease (Dow Corning) was used to provide lubrication and a seal around the slides. During testing air was used to activate the valve, and water was the fluid in chamber 2.

II. ANALYSIS

The object of this study was to determine the dynamic characteristics of this valve, for the purpose of obtaining a better understanding of the effects of geometry and pressure levels on its performance. Hopefully this will in the end lead to a better or more nearly optimum design.

The analytical model and nomenclature which was chosen is shown in Fig. II. Note that slide A is not shown. This was done for two reasons; first that the interesting part of the entire sequence of events happens after this slide has completed its motion, and, second, that it would not be possible to combine the analysis of the two slides without a delay function, a messy mathematical concept. The analysis consisted, then, of the dynamic characteristics of slide B after slide A had completed its motion.

Assuming that the damping between the slide and its container walls is completely viscous or proportional to the velocity with no static effects, Newton's second law gives for the slide

$$P_1A_1 - P_2A_2 = M\ddot{X} + B\dot{X} \tag{1}$$

The continuity equation applied to chamber 2 gives

$$Q_T = \text{Volume Flow Rate} = A_2\dot{X} \tag{2}$$

neglecting any compressibility effects. With the assumptions that the flow is fully developed and laminar with negligible entrance and exit effects, Ref. 1 says that

$$Q_T = \frac{A_T^2}{8\mu L}(P_2 - P_3) \tag{3}$$

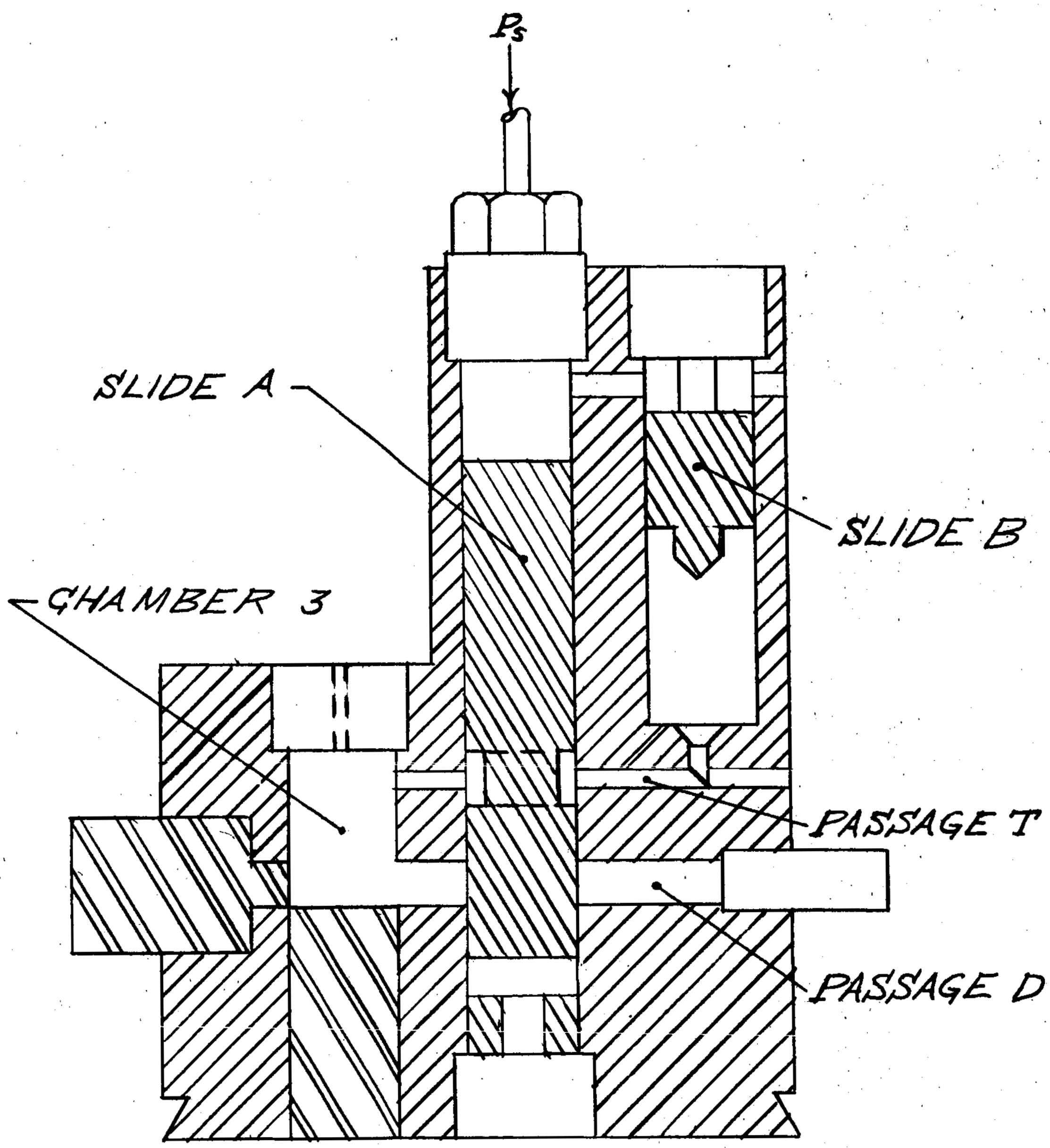

FIG. 1

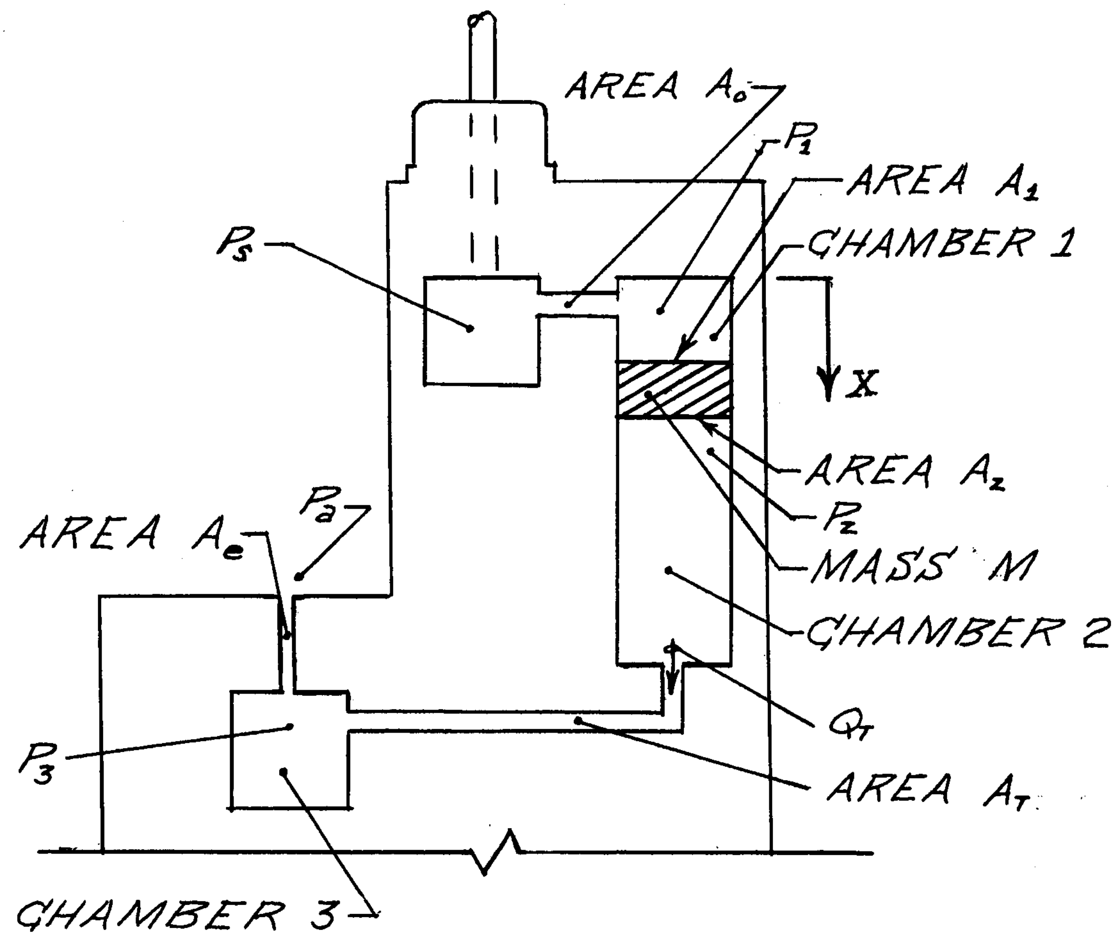
AREA A_o
P_1
AREA A_1
CHAMBER 1
P_s
X
AREA A_2
P_2
MASS M
AREA A_e
P_a
CHAMBER 2
Q_T
P_3
AREA A_T
CHAMBER 3

FIG. 2

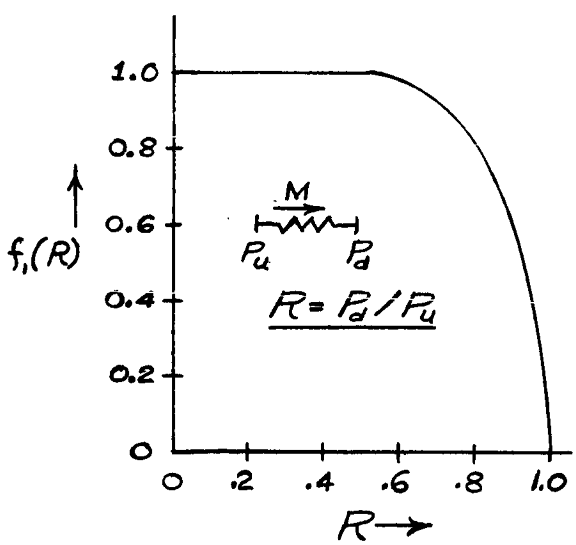
1.0
0.8
0.6
0.4
0.2
0
$f_1(R)$
M
P_u
P_d
$R = P_d / P_u$
0
.2
.4
.6
.8
1.0
R

FIG. 3

where μ is the fluid viscosity and L is the length of the tube.

For chambers 1 and 3 the continuity equation is

$$M_n = \text{Mass Flow Rate} = \frac{d}{dt}\left(\frac{P_n V_n}{R T_n}\right) \quad n=1,3 \tag{4}$$

and the energy equation is

$$M_n T_n - \frac{P_n}{c_p}\frac{dV_n}{dt} = \frac{1}{kR}\frac{d}{dt}(P_n V_n) \qquad n=1,3 \tag{5}$$

If the flow through passages A_o and A_e is assumed to be described by the orifice equation for compressible flow, M_1 can be related to P_1. For the area A_o

$$M_1 = C_{d1} C_B A_o P_s (T_s)^{-1/2} f_1\left(\frac{P_1}{P_s}\right) \tag{6}$$

where

$$f_1\left(\frac{P_1}{P_s}\right) = \frac{C_A}{C_B}\left(\frac{P_1}{P_s}\right)^{1/k}\left[1-\left(\frac{P_1}{P_s}\right)^{\frac{k-1}{k}}\right]^{1/2} \tag{7}$$

In this equation k is the ratio of specific heats (1.4 for air), C_a and C_b are constants, and C_{d1} is the discharge coefficient for the orifice. A similar equation could be written for M_3, and it would be possible to relate the motion of the slide to the pressure in chamber 3 and the exit pressure. As can be seen by an inspection of Eqn. 7 this relation would not be explicit and would be quite non-linear.

In order to obtain a representation suitable for analysis, a bit of linearization is now called for. It it is assumed that the change of state of the fluid in chamber 1 is isothermal, then for small variations

$$\Delta M_1 = \frac{1}{R T_{1i}}\left[P_{1i}\frac{d}{dt}(\Delta V_1) + V_{1i}\frac{d}{dt}(\Delta P_1)\right] \tag{8}$$

where the delta notation refers to a small change of the variable. The subscript i indicates that the quantity so marked is a constant evaluated at the operating point. If the change of state of the fluid is assumed to be adiabatic Eqn. 7 becomes

$$\Delta M_1 = \left[\frac{P_{1i}}{c_p T_1} + \frac{P_{1i}}{T_1 kR}\right]\frac{d(\Delta V_1)}{dt} + \frac{V_{1i}}{T_1 kR}\frac{d}{dt}(\Delta P_1) \tag{9}$$

It can be seen that the two equations are essentially the same, the only difference being in the magnitude of their constant coefficients. Rather than assuming one or the other, express the equation as

$$\Delta M_1 = C_1 \frac{d}{dt}(\Delta V_1) + C_2 \frac{d}{dt}(\Delta P_1) \tag{10}$$

A decision as to what type of conditions actually occur can then be put off until later, and the coefficients evaluated correspondingly. A similar analysis applied to chamber 3 gives

$$\Delta M_3 = C_3 \frac{d}{dt}(\Delta V_3) + C_4 \frac{d}{dt}(\Delta P_3) \tag{11}$$

The mass flow rate into chamber 1 is now found by linearizing Eqn. 6. If the assumption of constant supply pressure and temperature is made, this equation becomes

$$\Delta M_1 = \frac{\partial M_1}{\partial P_1}\Big/_i \Delta P_1 = C_5 \Delta P_1 \tag{12}$$

Correspondingly, for the mass flow rate out of chamber 3 it is found that

$$\Delta M_3 = \frac{\partial M_3}{\partial P_3}\Big/_i \Delta P_3 = C_6 \Delta P_3 \tag{13}$$

Linearization of Eqns. 1, 2, and 3 gives

$$\Delta P_1 A_1 - \Delta P_2 A_2 = M D^2(\Delta X) + B D(\Delta X) \tag{14}$$

$$\Delta Q_T = A_2 D(\Delta X) \tag{15}$$

$$\Delta Q_T = \frac{A_T^2}{8 \mu L}(\Delta P_2 - \Delta P_3) \tag{16}$$

where D = d/dt, the differential time operator. The change in volume, ΔV_1 and ΔV_2 may be expressed in terms of as

$$\Delta V_1 = A_1(\Delta X) \tag{17}$$

and

$$\Delta V_3 = -A_2(\Delta X) \tag{18}$$

Combining Eqns 10 through 18 it is found that

$$\left[M_2 D^2 + \left\{\frac{8\mu L A_2^2}{A_T^2} + B - \frac{C_1 A_1^2}{(C_5 - C_2 D)} + \frac{C_3 A_3 A_2}{(C_6 + C_4 D)}\right\} D\right] \Delta X = 0 \tag{19}$$

Some physical significance may now be attached to the coefficients. From the first term of the coefficient of the first order derivative it can be seen that the effective damping is directly proportional to the viscosity of the fluid and the length of passage T and inversely proportional to the square of the area of the passage. This seems logical and probably could have been assumed before the start of the analysis. The interesting part is that it is directly proportional to the square of the area of slide B, a result which is not so obvious.

The third term of this coefficient looks at first like a negative damping term. The coefficient C_1 comes from the equation of state of chanber 1, Eqn. 8, and is

$$C_1 = \frac{P_{1i}}{\mathcal{R} T_{1i}} \tag{20}$$

It is a positive quantity and so the full term still appears negative. In the denominator the term C_5 comes from the orifice equation, Eqn. 6. Performing the indicated differentiations it is found that

$$C_5 = \left\{ \left[\frac{.532\, C_{d_1} A_o C_B}{\sqrt{T_S}} \right] \left(\frac{\partial f_1}{\partial R} \right) \right\}_i \tag{21}$$

where

$$R = \frac{P_1}{P_S} \tag{22}$$

Figure 3 shows a plot of $f_1(R)$ versus R. As can be seen C_5 is just a multiple of the slope of this graph near the operating point. This will be a negative quantity. It should also be noted that for a small pressure drop across the orifice, i.e. $R \approx 1$, $\partial f_1/\partial R$ will be a large negative quantity.

The other term of the denominator, C_2, comes from the equation of state for chamber 1, Eqn. 8, and is equal to

$$C_2 = \frac{V_{1i}}{\mathcal{R} T_{1i}} \tag{23}$$

which is a positive quantity. Therefore the entire denominator will be negative, and so, cancelling this sign with the sign before the equation, it can be seen that the term in actuality applies positive damping to the system. (Reassurance as to the correctness of the analysis - negative damping could prove distressing.)

Performing a similar analysis of the last term of the coefficient it is found that the coefficient C_3 resembles C_1, being composed of the pressure P_3 and the temperature T_3. Also, correspondingly, C_4 resembles C_2 with the subscripts changed from 1 to 3. The interesting quantity in this case is C_6. Returning to Eqns. 13 and 6 and performing the indicated differentiations it is found that

$$C_6 = \left\{\left[\frac{.532\, C_{D3} A_e C_B}{\sqrt{T_3}}\right]\left[f_1(Q) - Q\,\frac{\partial f_1(Q)}{\partial Q}\right]\right\}_i \qquad (24)$$

where

$$Q = P_a / P_3 \qquad (25)$$

Applying the same reasoning as before and noting that f_1 and Q are positive quantities while $\partial f_1/\partial Q$ is a negative quantity we see that C_6 is a positive quantity. Therefore the entire last term is positive and contributes positive damping to the system.

The total damping coefficient is the composed of a number of effects. It could be broken down into four categories:

1. Damping due to viscous shear in the sealing grease
2. Damping due to the area of the passage T and the fluid which is being used
3. Damping due to orifice 1 and chamber volume 1
4. Damping due to orifice 3 and chamber volume 3

To get an idea of the relative magnitude of these terms a few values for the present operating point and present geometrical dimensions were used. Assuming

Supply pressure (P_s)	20 psig
Exit pressure (P_a)	15 psi
$A_1 = A_2 = A_3$	0.0708 in^2
A_t	0.0021 in^2
L	0.85 in
μ	2.71 lbm/hr ft
R	~ 1
Q	~ 1

calculations show that the equation of motion, expressed in numerical form is

$$6\times10^{-3} D^2 \Delta X + \left[2.83\times10^{-3} + 53.2 + \frac{3.9\times10^{-10}}{(\infty + 1.93\times10^{-10} D)} + \frac{1.7\times10^{-10}}{(\infty + .96\times10^{-10} D)}\right] D\Delta X$$

if the change of state is assumed isothermal and

$$6\times10^{-3} D^2 \Delta x + \left[2.83\times10^{-3} + 53.2 + \frac{9.8\times10^{-10}}{(\infty + 1.9\times10^{-10} D)} + \frac{1.7\times10^{-10}}{(\infty + .96\times10^{-10} D)}\right] D\Delta X$$

if it is considered adiabatic.

As can be seen, for the present operating point the contributions of the last two terms are negligible, irrespective of the assumed change of state. Apparently they will only be important under choked conditions. Under choked or near choked conditions $C_5 \rightarrow 0$ and $C_6 \rightarrow 1$. Therefore it appears that for all conditions the contribution due to the last term will be negligible. As stated before this is the contribution due to orifice 3 and volume 3. However, under choked conditions the contribution due to orifice 1 and volume 1 will not be a damping effect but rather a spring effect. An inspection of equations 20 and 23 show that the magnitude of this contribution will be directly proportional to the pressure P_1.

III. CONCLUSIONS

As expected the behavior of the valve is a damped-mass system under most conditions. The most important contribution to the damping term cones, as expected, from viscous shear with the sealing grease around the slide. The only other signigicant contribution comes from the dimensions of the passage T and the properties of the fluid contained in chamber 2. Under certain conditions, i.e. choked flow in orifice A_o, a spring force term will be introduced into the equation.

From this linearized analysis of slide B it is possible to draw a number of conclusions about the entire system. As the volume flow rate into chamber 3 is directly proportional to the displacement of the slide, knowing how this quantity varies will give us the flow rate for any conditions of geometry, fluid properties, and operating point. If the total time of action of the valve is of interest the action of slide A may be taken into account by merely considering it as a separate entity. The time required for its motion could then be added to the time of action of slide B for the total action time of the valve.

LIST OF REFERENCES

1. Blackburn, J.F., Reethof, G., and Shearer, J. L., Fluid Power Control, The Technology Press of M.I.T., Cambridge, Mass., 1960.

2. Keenan, J.H., and Kaye, J., Gas Tables, John Wiley and Sons, Inc., New York, 1950.

3. Shapiro, Ascher H., The Dynamics and Thermodynamics of Compressible Fluid Flow, Volume I , The Ronald Press, New York, 1953.